# $W = 0$ pairing in Hubbard and related models of low-dimensional superconductors



2004 J. Phys.: Condens. Matter 16 R1387

(http://iopscience.iop.org/0953-8984/16/47/R01)

INSTITUTE OF PHYSICS PUBLISHING JOURNAL OF PHYSICS: CONDENSED MATTER

J. Phys.: Condens. Matter **16** (2004) R1387–R1422 PII: S0953-8984(04)68289-0

**TOPICAL REVIEW**

# $W = 0$ pairing in Hubbard and related models of low-dimensional superconductors

**Adalberto Balzarotti**[1], **Michele Cini**[1,2,4], **Enrico Perfetto**[1,2] **and Gianluca Stefanucci**[3]

[1] Istituto Nazionale per la Fisica della Materia, Dipartimento di Fisica, Università di Rome Tor Vergata, via della ricerca Scientifica 1, 00133 Roma, Italy
[2] INFN—Laboratori Nazionali di Frascati, Via E Fermi 40, 00044 Frascati, Italy
[3] Department of Solid State Theory, Institute of Physics, Lund University, Sölvegatan 14 A, 22362 Lund, Sweden

Received 29 March 2004, in final form 7 October 2004
Published 12 November 2004
Online at stacks.iop.org/JPhysCM/16/R1387
doi:10.1088/0953-8984/16/47/R01

**Abstract**

Lattice Hamiltonians with on-site interaction $W$ have $W = 0$ solutions, that is, many-body *singlet* eigenstates without double occupation. In particular, $W = 0$ pairs give a clue to understand the pairing force in repulsive Hubbard models. These eigenstates are found in systems with high enough symmetry, like the square, hexagonal or triangular lattices. By a general theorem, we propose a systematic way to construct all the $W = 0$ pairs of a given Hamiltonian. We also introduce a canonical transformation to calculate the effective interaction between the particles of such pairs. In geometries appropriate for the $CuO_2$ planes of cuprate superconductors, armchair carbon nanotubes, or cobalt oxide planes, the dressed pair becomes a bound state in a physically relevant range of parameters. We also show that $W = 0$ pairs quantize the magnetic flux as superconducting pairs do. The pairing mechanism breaks down in the presence of strong distortions. The $W = 0$ pairs are also the building blocks for the antiferromagnetic ground state of the half-filled Hubbard model at weak coupling. Our analytical results for the $4 \times 4$ Hubbard square lattice, compared to available numerical data, demonstrate that the method, besides providing an intuitive grasp on pairing, also has quantitative predictive power. We also consider including phonon effects in this scenario. Preliminary calculations with small clusters indicate that vector phonons hinder pairing while half-breathing modes are synergic with the $W = 0$ pairing mechanism both at weak coupling and in the polaronic regime.

[4] Author to whom any correspondence should be addressed.

  

## Contents



## 1. Introduction

In the last decades, much effort has been devoted to *exotic* mechanisms of pairing and to the possibility of non-conventional superconductivity in new materials. In a list of the most important and frequently discussed examples, one could mention the cuprates [1], organic superconductors including fullerenes [2] and carbon nanotubes [3], ruthenates [4], and Na–Co oxides [5]. Among the most interesting possibilities, correlation effects have been invoked, and the Hubbard model [6] has been increasingly popular to achieve a simplified picture.

The Hubbard model is believed to exhibit various interesting phenomena including antiferromagnetism, ferrimagnetism, ferromagnetism, metal–insulator transitions, etc. It is the simplest Hamiltonian covering both aspects of a strongly correlated electron system (like the $CuO_2$ planes of cuprates), namely the competition between band-like behaviour and the tendency to atomic-like localization driven by the screened Coulomb repulsion. Besides, several authors believe that it can exhibit a superconducting phase in a certain parameter regime. Despite its simplicity, the Hubbard Hamiltonian cannot be exactly solved in more than 1D and a large variety of approaches has been proposed to study the superconducting correlations in the ground state and at finite temperature. Bickers and co-workers [7] were among the first to propose the $d_{x^2-y^2}$ wave superconductivity in 2D. A recent survey of the superconducting properties of the single- and multi-band Hubbard model can be found in [8].

Another popular class of models is that obtained from the Hubbard Hamiltonian in the strong-coupling limit. A large on-site Coulomb repulsive energy $U$ between carriers of opposite spins tends to reduce the double occupancy. A straightforward perturbation theory in the parameters $t$ of the kinetic term leads to Heisenberg-like Hamiltonians for fermions

propagating through an antiferromagnetic background with an exchange interaction $J$ between neighbouring spins. These are the so called $t$–$J$ models [9, 10]. In the $t$–$J$ model the double occupancy is forbidden by the so-called Gutzwiller projection [11], and there is no on-site repulsion. However, superconductivity is a delicate phenomenon and the exclusion of doubly occupied sites costs kinetic energy, so the $t$–$J$ model might fail to give an appropriate description of the Hubbard model when $U$ is comparable to $t$.

In this review article, we illustrate the '$W = 0$' pairing mechanism, in which symmetry is capable of cutting down the on-site repulsion from the outset, without any need of the Gutzwiller projection. This effect works at any $U/t$ and it relies on a configuration mixing which entails the presence of degenerate one-body states at the Fermi level. Moreover, we provide evidence that this configuration mixing, when applied to the full many-body problem, can produce pairing when physical parameter values are used.

The pairing force in the Hubbard model is induced by repulsive interactions, and recalls the Kohn–Luttinger [12] pairing in the jellium. They pointed out that any three-dimensional Fermi liquid undergoes a superconducting instability by Cooper pairs of parallel spins and very large relative angular momentum $l$. A simplified view of the Kohn–Luttinger effect is given by considering one particle of the pair as an external charge. Then, the screening gives rise to a long-range oscillatory potential (Friedel oscillations) due to the singularity of the longitudinal dielectric function at $2k_F$; here, $k_F$ is the Fermi wavevector. The strict reasoning exploits the fact that the Legendre expansion coefficients of any regular direct interaction between particles of opposite momentum drops off exponentially in $l$. On the other hand, the second-order contribution to the scattering amplitude falls as $1/l^4$ and at least for odd $l$ leads to an attractive interaction. In the modern renormalization group language [13], the second-order correction is obtained by summing up the marginal scattering amplitudes of the isotropic Fermi liquid coming from the so-called forward channels, including, for antiparallel spins, a spin-flip diagram. This scenario does not work in the two-dimensional Fermi liquid, but going beyond the second-order perturbation theory the Kohn–Luttinger effect is recovered [14].

The present mechanism works with singlet pairs and differs from the Kohn–Luttinger one in other important ways. In contrast with the homogeneous electron gas, the lattice structure gives very tight pairs and the $W = 0$ mechanism is displayed very clearly in tiny clusters as well. On top of that, it is worth noticing that in high-$T_C$ superconductors the size of the Cooper pairs is expected to be of the order of few lattice constants and hence the pairing mechanism should lend itself to cluster studies. Macroscopically large lattices with periodic boundary conditions have large symmetry groups including the space groups (point symmetry + translational symmetry); in such conditions, the $W = 0$ pairing mechanism is at its best. Similarly, in finite geometries, the largest binding energy is obtained in fully symmetric clusters while static distortions tend to unbind the pair. Exact calculations on finite models should bring to light interesting aspects of the microscopic origin of the pairing mechanism, and be useful as tests for the analytic developments.

To test the superconducting nature of the pairs arising from repulsive interactions, one can use finite systems in gedanken experiments. We probe the behaviour of $W = 0$ pairs in the presence of a static magnetic field and we show that they produce diamagnetic supercurrents that screen the vector potential. As a result the superconducting flux quantization is observed in various geometries.

The review is organized as follows. In section 2, we review the pairing mechanism in small symmetric clusters. We prove the existence of two-body singlet eigenstates with vanishing on-site Hubbard repulsion, that we call $W = 0$ pairs. We have collected in section 2.2 the somewhat more technical aspects, which are central for the mathematical foundation of the theory, while readers who are only interested in the phenomenology might skip it. We prove

a general theorem on the allowed symmetries of such pairs. From the theorem we extract a practical recipe to build $W = 0$ pairs in any symmetric geometry (finite or macroscopically large). A careful analysis on the smallest 'allowed' cluster, the $CuO_4$, shows that pairing can be obtained in a physical parameter range. The underlying pairing mechanism is investigated using many-body perturbation theory. In section 3 we generalize the theory to arbitrary large systems. We introduce a non-perturbative canonical transformation leading to an effective Hamiltonian for the pair. The method is free from the limitations of perturbation theory; the relation of the present formalism to Cooper theory from one side and to cluster results from the other is discussed. Two kinds of bound states of different symmetries result, and the dependence of the binding energy on the filling and other parameters is explored. In section 4 we study the Hubbard model at half filling. We remove the ground-state degeneracy in first order perturbation theory by means of a suitable *local* formalism. We show that the ground state is the spin singlet projection of a determinantal state exhibiting the *antiferromagnetic property*: the translation by a lattice step is equivalent to a spin flip. As an illustration, the $4 \times 4$ square lattice is studied in detail. The half filled antiferromagnetic ground state is doped with two holes and an effective interaction between them is derived by means of the canonical transformation. The analytical results agree well with the numerical ones and this shows the predictive power of the approach. In section 5 we investigate the $W = 0$ pairing mechanism in carbon nanotubes and triangular cobalt oxides. Section 6 is aimed to study the superconducting magnetic response of symmetric Hubbard models with $W = 0$ bound pairs. Section 7 deals with the inclusion of the lattice degrees of freedom; we show that phonons give a synergic contribution to the purely electronic mechanism and catastrophic Jahn–Teller distortions do not occur. Finally, we present our conclusions and outlook in section 8.

## 2. Pairing in the Hubbard model

In this review, we shall deal with Hubbard models of various geometries, designed for application to superconducting strongly correlated materials. The prototype Hubbard Hamiltonian reads

$$H = K + W = t \sum_{\langle i,j\rangle,\sigma} c^{\dagger}_{j\sigma} c_{i\sigma} + U \sum_{i} n_{i\uparrow} n_{i\downarrow}, \tag{1}$$

where $K$ stands for the kinetic energy while $W$ accounts for the on-site repulsive interaction. The summation on $\langle i, j\rangle$ runs over sites $i$ and $j$ which are nearest neighbours.

In equation (1) the interaction term is repulsive and there is no electron–phonon coupling, so the very existence of pairing is a paradox. An effective attractive force comes from, e.g., the exchange of spin fluctuations but it must be stronger than the direct Hubbard repulsion to give rise a bound pair. Bickers and co-workers [7] explored the consequences of a spin density wave instability on such a pairing force within the RPA approximation. They found a superconducting phase with pair-wavefunctions of $d_{x^2-y^2}$ symmetry in the 2D Hubbard model. The next level of calculations was carried out by using the FLEX approximation [15]. This method treats the fluctuations in the magnetic, density and pairing channels in a self-consistent and conserving way. It was found that the antiferromagnetic fluctuations lead to a superconducting phase of $d_{x^2-y^2}$ symmetry which neighbours the SDW phase, in accordance with the previous findings.

The phase diagram becomes less clear close to half filling because of the numerous infrared divergencies due to the nesting of the Fermi surface and Van Hove singularities. As a consequence, the results of any many-body treatment depend on the choice of diagrams to be summed. Renormalization group (RG) methods [13] are a well controlled alternative approach

to deal with Fermi systems having competing singularities. The RG has been used by several authors [16–18] to study the coupling flows at different particle densities. In agreement with the previous findings, RG calculations show a d-wave superconducting instability away from half filling. The underlying physical mechanism, namely exchange of spin- or charge-density fluctuations, is also the same as in the FLEX approach.

Despite such evidence, there is no general agreement on the existence of a superconducting phase in the Hubbard model [19–21]. In order to clarify such a controversy it is very useful to have exact data to rely on. Unfortunately, the one-band Hubbard model is exactly solved only in one spatial dimension [22] and no sign of superconductivity was found there[5]. Very few exact analytical results are available for the two-dimensional case[6]. Therefore, in two dimensions the low-lying states must be explored by means of exact diagonalizations on finite clusters. This kind of numerical calculation, complemented by analytical work and physical insight, may bring to light interesting local aspects of the microscopic pairing mechanism.

The exact ground states of several small Hubbard systems have been numerically found by means of Lanczos and quantum Monte Carlo techniques. A pairing criterion that we shall discuss below was given by Richardson in the context of nuclear physics [27]. Defining

$$\tilde{\Delta}(N+2) = E(N+2) + E(N) - 2E(N+1) \tag{2}$$

where $E(N)$ is the $N$-body ground-state energy,

$$\tilde{\Delta}(N+2) < 0 \tag{3}$$

signals a bound pair in the ground state with $N+2$ particles and $|\tilde{\Delta}|$ is interpreted as the binding energy of the pair. Pairing was found under various conditions by several authors [28, 29], and among the geometries considered the $4 \times 4$ system [30] is one of the most relevant for studying the pairing instability close to the antiferromagnetic phase.

Below, we derive an analytic theory of pairing interactions, and report several detailed case studies where the formulae are validated by comparison with the numerical data. The results support general qualitative criteria for pairing induced by the on-site repulsion only. This shows that our approach successfully predicts the formation of bound pairs, and explains why other ingredients like strong off-site interactions are needed in other geometries. The analytic approach is also needed to predict what happens for large systems and in the thermodynamic limit. Increasing the cluster size the computed pair binding energies show a rapid decrease, and several authors on the basis of the numerical data consider pairing in the Hubbard model as a size effect. Unfortunately, the number of configurations grows in a prohibitive way with the cluster size[7] and numerical data currently available on $4 \times 4$ or even $6 \times 6$ clusters cannot provide reliable extrapolations to the bulk limit. In section 3.4 we show that we understand the trend analytically very well, that much larger cells (at least $30 \times 30$) are needed to estimate the asymptotic behaviour, and that we have reason to believe that pairing with a reduced but substantial binding energy persists in the full plane.

### *2.1. $W = 0$ pairing in Cu–O clusters*

In this section, we illustrate the concept of $W = 0$ pairs and the way they become bound states, by using examples with a geometry relevant for the cuprates. Our starting point is the

[5] The Hubbard chain is classified as a Mott insulator with a spin gap at half-filling and as a Luttinger liquid away from it.

[6] Among them we mention the theorems by Lieb [23], on the ground-state spin degeneracy at half filling, the ferromagnetic ground-state solutions devised by Nagaoka [24], Mielke [25], and Tasaki [26], and the extensions of the Mermin–Wagner theorem on the absence of long-range order at finite temperature, provided by Su and Suzuki [21].

[7] The $4 \times 4$ model is the largest square Hubbard system where exact diagonalizations have been performed; indeed, the Hilbert space contains $166 \times 10^6$ configurations!

**Table 1.** Character table of the $C_{4v}$ symmetry group. Here **1** denotes the identity, $C_2$ the 180° rotation, $C_4^{(+)}, C_4^{(-)}$ the anticlockwise and clockwise 90° rotation, $\sigma_x, \sigma_y$ the reflection with respect to the $y = 0$ and $x = 0$ axis, and $\sigma_+, \sigma_-$ the reflection with respect to the $x = y$ and $x = -y$ diagonals. The $C_{4v}$ symmetry group has four one-dimensional irreducible representations (irreps), $A_1$, $A_2$, $B_1$, $B_2$, and one two-dimensional irrep, $E$. In the last column it is shown how each of them transforms under $C_{4v}$.

| $C_{4v}$ | **1** | $C_2$ | $C_4^{(+)}, C_4^{(-)}$ | $\sigma_x, \sigma_y$ | $\sigma_+, \sigma_-$ | Symmetry |
|---|---|---|---|---|---|---|
| $A_1$ | 1 | 1 | 1 | 1 | 1 | $x^2 + y^2$ |
| $A_2$ | 1 | 1 | 1 | −1 | −1 | $(x/y) - (y/x)$ |
| $B_1$ | 1 | 1 | −1 | 1 | −1 | $x^2 - y^2$ |
| $B_2$ | 1 | 1 | −1 | −1 | 1 | $xy$ |
| $E$ | 2 | −2 | 0 | 0 | 0 | $(x, y)$ |

three-band Hubbard Hamiltonian

$$H = K + W + W_{\text{off-site}} \tag{4}$$

where

$$K = t \sum_{\langle ij\rangle,\sigma} (p^\dagger_{j\sigma} d_{i\sigma} + \text{h.c.}) + t_{pp} \sum_{\langle jj'\rangle,\sigma} p^\dagger_{j\sigma} p_{j'\sigma} + \varepsilon_{\text{d}} \sum_{i,\sigma} n_{i\sigma} + \varepsilon_{\text{p}} \sum_{j,\sigma} n_{j\sigma}$$

and

$$W = U_{\text{d}} \sum_i n_{i\uparrow} n_{i\downarrow} + U_{\text{p}} \sum_j n_{j\uparrow} n_{j\downarrow}, \qquad W_{\text{off-site}} = U_{\text{pd}} \sum_{\langle ij\rangle,\sigma\sigma'} n_{i\sigma} n_{j\sigma'}.$$

Here, $p_j$ ($d_i$) are fermionic operators that destroy holes at the oxygen (copper) ions labelled $j$ ($i$) and $n = p^\dagger p$ ($= d^\dagger d$) is the number operator. $\langle ij\rangle$ refers to pairs of nearest-neighbour $i$ (copper) and $j$ (oxygen) sites. The hopping terms correspond to the hybridization between nearest-neighbour Cu and O atoms, and are roughly proportional to the overlap between localized Wannier orbitals.

The parameters $U_{\text{d}}$ and $U_{\text{p}}$ are positive constants that represent the repulsion between holes when they are at the same copper (d) and oxygen (p) orbitals, respectively. $U_{\text{pd}}$ has a similar meaning, i.e., it corresponds to the Coulombic repulsion when two holes occupy two adiacent Cu–O sites. The on-site energies $\varepsilon_{\text{p}}$ and $\varepsilon_{\text{d}}$ refer to the occupied orbitals of oxygen and copper. In the strong-coupling limit, and with one particle per unit cell, this model reduces to the spin Heisenberg model with a superexchange antiferromagnetic coupling [36, 37].

From a band structure calculation and by best fitting the results of *ab initio* calculations [38] one can roughly estimate the actual values of the parameters in the Hamiltonian of equation (4). Our preferred set is (in eV): $\varepsilon_{\text{p}} - \varepsilon_{\text{d}} = 3.5$, $t = 1.3$, $t_{pp} = -0.65$, $U_{\text{d}} = 5.3$, $U_{\text{p}} = 6$ and, most probably, $U_{\text{pd}} < 1.2$.

As Cini and Balzarotti [31] pointed out, highly symmetric clusters possess two-hole singlet eigenstates of $H$ which do not feel the on-site repulsion $W$; such eigenstates were called $W = 0$ *pairs* and play a crucial role for pairing. In order to have $W = 0$ solutions, the clusters must possess the full $C_{4v}$ (square) symmetry, and must be centred around a Cu site. Group arguments are central to our approach and we show the characters of the $C_{4v}$ group in table 1. The symmetry requirements are so stringent that clusters with such properties had not been studied previously. In particular, the present discussion does not apply to the geometries, like those examined by Hirsch *et al* [32, 33] and Balseiro *et al* [28], which are *forbidden* from our viewpoint. The $Cu_4O_4$ geometry considered by Ogata and Shiba [34] has the $C_{4v}$ symmetry, but lacks the central Cu, and therefore it is *forbidden*. Those built from degenerate one-body

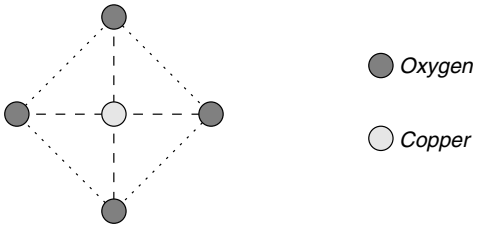


**Figure 1.** The topology of the $CuO_4$ cluster.

**Table 2.** One-body levels of the $CuO_4$ cluster in units of $t$ as a function of the dimensionless parameter $\tau \equiv t_{pp}/t$.

| $\varepsilon_{A_1}$ | $\varepsilon_{E_x}$ | $\varepsilon_{E_y}$ | $\varepsilon_{B_1}$ | $\varepsilon_{A_1'}$ |
|---|---|---|---|---|
| $\tau - \sqrt{4+\tau^2}$ | 0 | 0 | $-2\tau$ | $\tau + \sqrt{4+\tau^2}$ |

levels are not $W = 0$ pairs; they feel the on-site repulsion $U_p$ on the oxygen sites, and yield $\tilde{\Delta} < 0$ only if $U_p$ is very small [31, 35].

Note that we are using the same $t$ for all Cu–O bonds, while some authors use other conventions. For instance, Zhang and Rice [39] use an alternating sign prescription for $t$, which may be obtained by changing the sign of all the O orbitals in the horizontal lines containing Cu ions. The two pictures are related by a gauge transformation, under which the orbital symmetry labels $A_1$ and $B_1$ are interchanged. Some of the symmetry related information is gauge dependent and unobservable, while some is physical (e.g. degeneracies are).

The reason why symmetry is so basic for our mechanism is that the $W = 0$ two-body eigenstates arise when two holes occupy degenerate one-body levels. When such degenerate states are partially filled in the many-body ground state, bound pairs can form. The *interacting ground state* must be described in terms of a many-body configuration mixing, but the presence of the $W = 0$ pair imparts to the many-body state a special character; it can be described in terms of a bound pair moving on a closed-shell background. This is the main point that we want to make, and it is deeply related to the symmetry quantum numbers.

The smallest square Cu–O cluster, $CuO_4$, see figure 1, is also the simplest where $W = 0$ pairing occurs. The Hamiltonian reads

$$H_{CuO_4} = t \sum_{i\sigma} (d_\sigma^\dagger p_{i\sigma} + p_{i\sigma}^\dagger d_\sigma) + t_{pp} \sum_{\langle ij\rangle,\sigma} p_{i,\sigma}^\dagger p_{j,\sigma} + U\left(n_\uparrow^{(d)} n_\downarrow^{(d)} + \sum_i n_{i\uparrow}^{(p)} n_{i\downarrow}^{(p)}\right). \tag{5}$$

The one-body levels and their symmetry labels are reported in table 2. Labelling the oxygen atomic sites by the numbers 1, 2, 3, 4, the diagonalizing creation operators are given by

$$\begin{aligned}
c_{E_y\sigma}^\dagger &= \frac{1}{\sqrt{2}}\left(p_{2\sigma}^\dagger - p_{4\sigma}^\dagger\right) \\
c_{E_x\sigma}^\dagger &= \frac{1}{\sqrt{2}}\left(p_{1\sigma}^\dagger - p_{3\sigma}^\dagger\right) \\
c_{B_1\sigma}^\dagger &= \frac{1}{2}\left(p_{1\sigma}^\dagger - p_{2\sigma}^\dagger + p_{3\sigma}^\dagger - p_{4\sigma}^\dagger\right) \\
c_{A_1\sigma}^\dagger(1) &= \frac{1}{\alpha_+^2 + 4}\left(\alpha_+ d_\sigma^\dagger + p_{1\sigma}^\dagger + p_{2\sigma}^\dagger + p_{3\sigma}^\dagger + p_{4\sigma}^\dagger\right) \\
c_{A_1\sigma}^\dagger(2) &= \frac{1}{\alpha_-^2 + 4}\left(\alpha_- d_\sigma^\dagger + p_{1\sigma}^\dagger + p_{2\sigma}^\dagger + p_{3\sigma}^\dagger + p_{4\sigma}^\dagger\right)
\end{aligned} \tag{6}$$

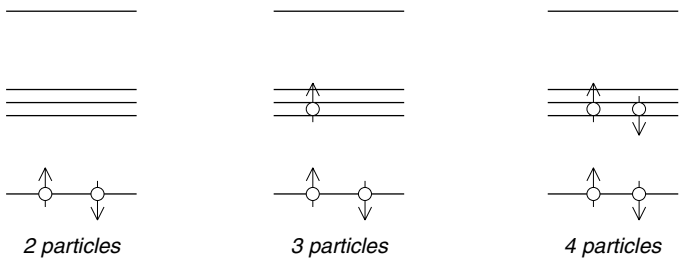


**Figure 2.** Many-body states for the $CuO_4$ cluster. For each number of particles is reported the component of highest weight of the ground state.

where $\alpha$ and $\beta$ depend on $\tau = t_{pp}/t$ as follows:

$$\alpha_{\pm} = \frac{4\left(\pm 1 \pm \tau^2 + \tau\sqrt{4+\tau^2}\right)}{\pm 5\tau \pm 2\tau^3 + \sqrt{4+\tau^2} + 2\tau^2\sqrt{4+\tau^2}}.$$

Let us build a four-hole state in the $CuO_4$ cluster in the non-interacting limit, according to the *aufbau* principle (see figure 2). The first two holes go into a bonding level of $A_1$ symmetry; this is a totally symmetric ($^1A_1$) pair. For negative $\tau$, the other two holes go into a non-bonding level of $E(x, y)$ symmetry, which contains four spin–orbital states. The Pauli principle allows $\binom{4}{2} = 6$ different pair states. The irrep multiplication table allows for labelling them according to their space symmetry: $E \otimes E = A_1 \bigoplus A_2 \bigoplus B_1 \bigoplus B_2$. It is also straightforward to verify that $A_2$ is a spin triplet, $^3A_2$, while the remaining irreps are spin singlets, $^1A_1$, $^1B_1$ and $^1B_2$. From equation (6) one readily realizes that the $B_2$ singlet operator

$$b^{\dagger}_{B_2} = \frac{1}{\sqrt{2}}\left(c^{\dagger}_{E_x\uparrow}c^{\dagger}_{E_y\downarrow} + c^{\dagger}_{E_y\uparrow}c^{\dagger}_{E_x\downarrow}\right) \tag{7}$$

is a $W = 0$ pair (no double occupation). Note that $^1B_2$ is the symmetry label of the pair wavefunction in the gauge we are using, and must not be confused with the symmetry of the order parameter.

To first order in perturbation theory, the four-body singlet state of $B_2$ symmetry is degenerate with the $A_2$ triplet; Hund's rule would have predicted a $^3A_2$ ground state. However, the true ground state turns out to be singlet, for reasons that we shall study below. The numerical results on the $CuO_4$ cluster show that $\tilde{\Delta}(4)$ is negative for $0 > \tau > -0.5$ and that its minimum value occurs at $\tau = 0$, when the non-bonding orbitals $B_1$ and $E$ become degenerate: the paired interacting ground state is also degenerate in this particular case. A symmetry analysis of this accidental degeneracy is postponed to the next section. In figure 3 we plot $\tilde{\Delta}(4)$ for $\tau = 0$, $\varepsilon_p - \varepsilon_d = 0$, $U_{pd} = 0$ and $U_p = U_d = U$. $\tilde{\Delta}(4)$ has a minimum at $U \approx 5t$ and it is negative when $0 < U < 34.77t$. We emphasize that $\tilde{\Delta}(4)$ becomes positive for large values of $U/t$ and hence pairing disappears in the strong-coupling regime. In the present problem $U$ must exceed several tens of $t$ before the asymptotic *strong-coupling regime* sets in. A perturbation theory will strictly apply at *weak coupling* where the second derivative of the curve is negative. However, qualitatively a weak-coupling approach is rewarding in the whole physically interesting range of parameters. The sign of $\tilde{\Delta}$ depends on $U$ and $\tau$ and its magnitude is unlike any of the input parameters; below, we show that this new energy scale emerges from an interference between electron–hole exchanges of different symmetries.

On the other hand, at positive $\tau$ the $B_1$ non-bonding level is pushed below the degenerate one and $\tilde{\Delta}(4)$ becomes large and positive (at $\tau = +0.65$, $\tilde{\Delta}(4) = 0.53$ eV).

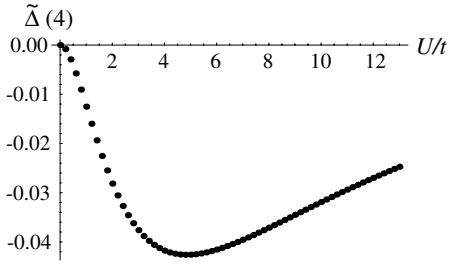


**Figure 3.** $\tilde{\Delta}(4)$ (in $t$ units) as a function of $U/t$. The maximum binding occurs at $U \sim 5t$ where $\tilde{\Delta}(4) \approx -0.042t$. For $U > 34.77t$ (not shown), $\tilde{\Delta}(4)$ becomes positive and pairing disappears.

Next, we discuss the dependence of $\tilde{\Delta}(4)$ on the other parameters [31]. If we decrease $\varepsilon_p$, $\tilde{\Delta}(4)$ decreases because this makes the system more polarizable. The $\varepsilon_p$ dependence when all the other parameters are kept fixed and $U_{pd} = 0$ is almost linear down to $\varepsilon_p = 0$. According to [28] positive $U_{pd}$ values do not spoil the mechanism, and tend to be synergic with it. Indeed, values of $U_{pd} > 0.6$ eV give negative $\tilde{\Delta}(4)$ values even for $\tau = -0.65$ eV (in the range 0.2–1.2 eV considered in [31] $\tilde{\Delta}(4)$ is a monotonically decreasing function of $U_{pd}$). Finally, we have numerically studied how the distortions affect $\tilde{\Delta}(4)$. We have found that any lowering of the symmetry is reflected by a corresponding increase of $\tilde{\Delta}(4)$ [31].

In the $CuO_4$ cluster we need four holes to have a paired ground state. Hence, the total hole concentration is $\rho_h = 0.8$. This value is too large by a factor of two with respect to the experimentally observed $\rho_h \simeq 0.4$ of the optimally doped systems. It is important to realize that these undesirable features are peculiar to the prototype $CuO_4$ cluster, and already disappear in $Cu_5O_4$, the next larger cluster of the same symmetry. In fact, four holes are still sufficient to reach degenerate states, but $\rho_h \sim 0.44$ is much closer to the experimental value. We have performed numerical explorations in other fully symmetric clusters like $Cu_5O_4$ and $Cu_5O_{16}$ and we have found negative values of $\tilde{\Delta}(4)$, of the order of few meV, using physical parameters. In all the allowed clusters up to 21 atoms, the lowest one-hole level belongs to $A_1$ symmetry, and the next $E$ level yields the $W = 0$ pair. The interactions produce a non-degenerate $^1B_2$ four-hole ground state *having the same symmetry as the* $W = 0$ *pair*. The interested reader may see [40, 41] for the details. Below, in section 3 we show [42] that the $\tilde{\Delta}(4) < 0$ arises from an effective attractive interaction between the holes of the $W = 0$ pair; the same interaction is repulsive for triplet pairs.

### 2.2. *Symmetry of the* $W = 0$ *pairs: a general theorem*

Since the mechanism depends on symmetry in such a fundamental way, we must refine the group theory analysis. We have discovered a powerful and elegant criterion [43] to construct all the $W = 0$ pair eigenstates on a given lattice $\Lambda$ by using projection operators.

Let $\mathcal{G}_0$ be the symmetry group of the non-interacting Hubbard Hamiltonian $K = \sum_{\langle ij\rangle,\sigma} t_{ij} c^\dagger_{j\sigma} c_{i\sigma}$. We assume that no degeneracy between one-body eigenstates is accidental, hence $\mathcal{G}_0$ must contain enough operations to justify all such degeneracies. Let us label each one-body eigenstate of $H = K + W$, $W = \sum_{i\in\Lambda} U_i n_{i\uparrow} n_{i\downarrow}$, with an irreducible representation (irrep) of $\mathcal{G}_0$.

**Definition.** An irrep $\eta$ is represented in the one-body spectrum of $H$ if at least one of the one-body levels belongs to $\eta$.

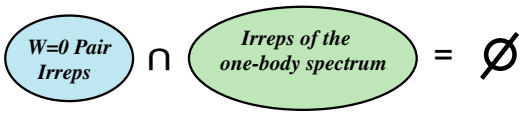


**Figure 4.** Schematic of the $W = 0$ theorem.
(This figure is in colour only in the electronic version)

Let $\mathcal{E}$ be the set of the irreps of $\mathcal{G}_0$ which are represented in the one-body spectrum of $H$. Let $|\psi\rangle$ be a two-body eigenstate of the non-interacting Hamiltonian with spin $S^z = 0$ and $P^{(\eta)}$ the projection operator on the irrep $\eta$. We wish to prove the following theorem.

$W = 0$ **Theorem.** *Any non-vanishing projection of $|\psi\rangle$ on an irrep not contained in $\mathcal{E}$ is an eigenstate of $H$ with no double occupancy. The singlet component of this state is a $W = 0$ pair. Conversely, any pair belonging to an irrep represented in the spectrum must have non-vanishing $W$ expectation value (see figure 4):*

$$\eta \notin \mathcal{E} \Leftrightarrow W P^{(\eta)} |\psi\rangle = 0. \tag{8}$$

**Remark.** Suppose we perform a gauge change in $H$ such that $\mathcal{G}_0$ is preserved; clearly, a $W = 0$ pair goes to another $W = 0$ pair. Thus, the theorem implies a distinction between symmetry types which is gauge independent.

**Proof.** Let us consider a two-body state of opposite spins belonging to the irrep $\eta$ of $\mathcal{G}_0$:

$$|\psi^{(\eta)}\rangle = \sum_{ij\in\Lambda} \psi^{(\eta)}(i, j) c^\dagger_{i\uparrow} c^\dagger_{j\downarrow} |0\rangle.$$

Then we have

$$n_{i\uparrow} n_{i\downarrow} |\psi^{(\eta)}\rangle = \psi^{(\eta)}(i, i) c^\dagger_{i\uparrow} c^\dagger_{i\downarrow} |0\rangle \equiv \psi^{(\eta)}(i, i) |i\uparrow, i\downarrow\rangle.$$

We define $P^{(\eta)}$ as the projection operator on the irrep $\eta$. Since

$$P^{(\eta)} \sum_{i\in\Lambda} \psi^{(\eta)}(i, i) |i\uparrow, i\downarrow\rangle = \sum_{i\in\Lambda} \psi^{(\eta)}(i, i) |i\uparrow, i\downarrow\rangle,$$

if $P^{(\eta)}|i\uparrow, i\downarrow\rangle = 0\ \forall i \in \Lambda$, then $\psi^{(\eta)}(i, i) = 0\ \forall i \in \Lambda$. It is worth noting that this condition is satisfied if and only if $P^{(\eta)}|i\sigma\rangle = 0\ \forall i \in \Lambda$, where $|i\sigma\rangle = c^\dagger_{i\sigma}|0\rangle$. Now it is always possible to write $|i\sigma\rangle$ in the form $|i\sigma\rangle = \sum_{\eta\in\mathcal{E}} c^{(\eta)}(i)|\eta_\sigma\rangle$ where $|\eta_\sigma\rangle$ is the one-body eigenstate of $H$ with spin $\sigma$ belonging to the irrep $\eta$. Hence, if $\eta' \notin \mathcal{E}$, $P^{(\eta')}|i\sigma\rangle = 0$ and so $P^{(\eta')}|i\uparrow, i\downarrow\rangle = 0$. Therefore, if $|\psi^{(\eta)}\rangle$ is a two-hole singlet eigenstate of the kinetic term and $\eta \notin \mathcal{E}$, then it is also an eigenstate of $W$ with vanishing eigenvalue, that means a $W = 0$ pair. □

The content of the theorem is schematically represented by figure 4.

We already know that $CuO_4$ is a good example of this theorem. Indeed, the irrep $B_2$ of the $W = 0$ pair is not represented in the spectrum (see table 2); $A_2$ is also not represented, but it yields no two-body states. This possibility is admitted by equation (8).

The particular case of $CuO_4$ with $\tau = 0$ is of special interest as an illustration. There is an *accidental* degeneracy between $E(x, y)$ and $B_1$ orbitals and therefore a three-times degenerate one-body level exists. With four interacting fermions, pairing occurs in two ways, as $A_1$ and $B_2$ are both degenerate ground states. This agrees with the theorem; in fact, the extra degeneracy cannot be explained in terms of $C_{4v}$, whose irreps have dimension two at most. For $\tau = 0$ any permutation of the four oxygen sites is actually a symmetry and therefore $\mathcal{G}_0$ is enlarged

to $S_4$ (the group of permutations of four objects). $S_4$ has the irreducible representations $\mathcal{A}_1$ (total symmetric), $\mathcal{B}_2$ (total antisymmetric), $\mathcal{E}$ (self-dual), $\mathcal{T}_1$, and its dual $\mathcal{T}_2$, of dimensions one, one, two, three, and three, respectively. These irreps break in $C_{4v}$ as follows:

$$\mathcal{A}_1 = A_1, \qquad \mathcal{T}_1 = B_1 \oplus E, \qquad \mathcal{T}_2 = A_2 \oplus E, \qquad \mathcal{B}_2 = B_2, \qquad \mathcal{E} = A_1 \oplus B_2.$$

Labelling the one-body levels with the irreps of $S_4$, one finds that $\mathcal{E}$ is not contained in the spectrum and thus yields $W = 0$ pairs:

$$^1\mathcal{E} = {}^1A_1 \ \oplus \ {}^1B_2. \tag{9}$$

The explicit expression of the corresponding pair-creation operators is

$$b^\dagger_{A_1} = \frac{2}{\sqrt{3}} c^\dagger_{B_1\uparrow} c^\dagger_{B_1\downarrow} + \frac{1}{\sqrt{3}} \left( c^\dagger_{E_x\uparrow} c^\dagger_{E_x\downarrow} + c^\dagger_{E_y\uparrow} c^\dagger_{E_y\downarrow} \right)$$

for the total-symmetric pair and equation (7) for the $B_2$ component.

In section 4.3 we shall show use the theorem with a $\mathcal{G}_0$ that includes symmetries which are not isometries. We shall see that this theorem puts useful restrictions on the many-body ground-state symmetry. The complete characterization of the symmetry of $W = 0$ pairs requires the knowledge of $\mathcal{G}_0$. A partial use of the theorem is possible if one does not know $\mathcal{G}_0$ but knows a subgroup $\mathcal{G}_0^<$. It is then still granted that any pair belonging to an irrep of $\mathcal{G}_0^<$ not represented in the spectrum has the $W = 0$ property. On the other hand, accidental degeneracies occur with a subgroup of $\mathcal{G}_0$, and by mixing degenerate pairs belonging to irreps represented in the spectrum one can also find $W = 0$ pairs there.

The theorem tells us that the *bigger* $\mathcal{G}_0$ is, the *larger* is the number of $W = 0$ pairs. Indeed, for a given system, the number of one-body eigenvectors is fixed, while the number and the dimension of the irreps grow with the order of the group. Therefore, the number of irreps not represented in $\mathcal{E}$ also grows, meaning more $W = 0$ pairs. At the same time, a big 'non-interacting' symmetry group $\mathcal{G}_0$ grants large level degeneracies. As we have seen, this fact allows the existence of $W = 0$ pairs formed by degenerate orbitals. In the next section we show that an anomalously low effective repulsion takes place in the interacting system when such levels are on the Fermi surface and that in a certain region of the parameter space this leads to pairing.

## 3. Theory of pairing in repulsive Hubbard models

In section 2 we have shown that $W = 0$ pairs may lead to a paired ground state in fully symmetric $C_{4v}$ clusters centred around a Cu ion. In this section we extend the theory to the full plane, and show that such pairs provide the natural explanation of the pairing instability of the Hubbard model. By a novel canonical transformation approach, we shall calculate the effective interaction $W_{\text{eff}}$ between two holes added to the ground state of the repulsive Hubbard model. Furthermore, we shall show that $W_{\text{eff}}$ is attractive in the $W = 0$ pair-symmetry channels. The method is a particularly efficient way to perform the configuration interaction calculation. It is based on the symmetry and sheds light on the origin of pairing in the $CuO_2$ plane. It is worth noticing that $W = 0$ pairs emerge from symmetry alone and hence remain $W = 0$ for any coupling strength $U$. This is the reason why weak-coupling expansions provide often good approximations at intermediate coupling as well, as observed by several authors [44–46].

### *3.1. $W = 0$ pairs in the planar Hubbard model*

The $CuO_2$ planes of cuprates have a large symmetry group which contains the space group $\mathcal{G} = T \otimes C_{4v}$, where $T$ is the group of translations and $\otimes$ stands for the semidirect product.

However, the optimal group $\mathcal{G}_0$ is much larger than $\mathcal{G}$.[8] For this reason, instead of using the $W = 0$ theorem, it is easier to follow the simple route of projecting a single determinantal state on the irreps of $C_{4v}$ [47, 48]. This partial use of the symmetry still gives enough solutions to demonstrate pairing.

Let us focus on $W = 0$ pairs with vanishing quasimomentum. Omitting band indices, we denote by

$$|d[\mathbf{k}]\rangle = c^{\dagger}_{\mathbf{k},\uparrow} c^{\dagger}_{-\mathbf{k},\downarrow} |0\rangle \tag{10}$$

a two-hole determinantal state, where $\mathbf{k}$ and $-\mathbf{k}$ label degenerate one-body eigenfunctions of $K$. The combination $|d[\mathbf{k}]\rangle + |d[-\mathbf{k}]\rangle$ is singlet and $|d[\mathbf{k}]\rangle - |d[-\mathbf{k}]\rangle$ is triplet. We introduce the determinants $|d[R\mathbf{k}]\rangle \equiv |d[\mathbf{k}_R]\rangle$, $R \in C_{4v}$, and the projected states

$$|\Phi_\eta[\mathbf{k}]\rangle = \frac{1}{\sqrt{8}} \sum_{R \in C_{4v}} \chi^{(\eta)}(R)\, |d[\mathbf{k}_R]\rangle \tag{11}$$

where $\chi^{(\eta)}(R)$ is the character of the operation $R$ in the irrep $\eta$.

In the three-band model we showed that $W = 0$ pairs are obtained by projecting onto the irreps[9] $A_2$ and $B_2$ (which are not represented in the one-body spectrum, as they should be). These irreps differ from those obtained in the fully symmetric clusters, where $W = 0$ pairs had $A_1$ and $B_2$ symmetry [49]. The reason for this change is a twofold size effect. On one hand, $A_1$ pairs have the $W = 0$ property only in clusters having the topology of a cross (whose symmetry group is $S_4$ rather than $C_{4v}$), but do not generalize as such to the full plane (when the symmetry is lowered to $C_{4v}$). On the other hand, the small clusters admit no $W = 0$ solutions of $A_2$ symmetry if only degenerate states are used.

We recall that a necessary condition for pairing in clusters is that the least bound holes form a $W = 0$ pair, and this dictates conditions on the occupation number. In the full plane, however, $W = 0$ pairs exist at the Fermi level for any filling. We also observe that the $W = 0$ pairs obtained with the above procedure are not *all* the possible $W = 0$ pairs in the one- and three-band Hubbard models, since the $W = 0$ theorem has not been fully exploited. However, it can be shown that they are the only $W = 0$ pairs with holes in degenerate one-body levels and with vanishing quasimomentum.

### *3.2. Canonical transformation*

In this section we intend to study the effective interaction $W_{\text{eff}}$ between the particles forming a $W = 0$ pair added to the $N$-body interacting ground state $|\Phi_U(N)\rangle$. Since the two extra particles cannot interact directly (by definition of the $W = 0$ pair), their effective interaction emerges from virtual electron–hole exchanges, and in principle can be attractive.

Many configurations contribute to the interacting $(N+2)$-body ground state $|\Phi_U(N+2)\rangle$ and we need a complete set $\mathcal{S}$ to expand it exactly; as long as it is complete, however, we can design $\mathcal{S}$ as we please. We can take the non-interacting $N$-body Fermi *sphere* $|\Phi_0(N)\rangle$ as our vacuum and build the complete set in terms of excitations over it. In the subspace with vanishing spin $z$ component, the simplest states that enter the configuration mixing are those obtained from $|\Phi_0(N)\rangle$ by creating two extra holes[10] over it; we denote these states by $|m\rangle$. Similarly, along with the pair $m$ states, we introduce the four-body $\alpha$ states, obtained

[8] Consider for instance that the largest irrep of the space group has dimension eight, while the half-filling shell is $2N - 2$ times degenerate, where $N \times N$ is the total number of unit cells in the system.

[9] Similarly, we have shown that the one-band Hubbard model admits $W = 0$ pairs belonging to the $A_2$, $B_1$ and $B_2$ irreps.

[10] For the sake of clarity we are assuming here that the particles we are considering are holes, as in cuprates; however, the canonical transformation is not limited to this case and it is applicable both to electrons and holes.

from $|\Phi_0(N)\rangle$ by creating two holes and one electron–hole (e–h) pair. Then, $\mathcal{S}$ includes the six-body $\beta$ states having two holes and two e–h pairs, and so on. We are using Greek indices for the configurations containing the electron–hole pairs, which here are playing largely the same role as phonons in the Cooper theory. By means of the complete set $\mathcal{S}$ we now expand the interacting ground state

$$|\Phi_U(N+2)\rangle = \sum_m a_m|m\rangle + \sum_\alpha a_\alpha|\alpha\rangle + \sum_\beta a_\beta|\beta\rangle + \cdots \tag{12}$$

and set up the Schrödinger equation

$$H|\Phi_U(N+2)\rangle = E|\Phi_U(N+2)\rangle.$$

We emphasize that equation (12) is a configuration interaction, *not a perturbative expansion*. When the number $N$ of holes in the system is such that $|\Phi_0(N)\rangle$ is a single non-degenerate determinant (the Fermi surface is totally filled), the expansion (12) for the interacting ground state is unique and we can unambiguously define and calculate the effective interaction $W_{\text{eff}}$. This is done by a canonical transformation [41, 47, 48] of the many-body Hubbard Hamiltonian. We consider the effects of the operators $K$ and $W$ on the terms of $|\Phi_U(N+2)\rangle$. Choosing the $m, \alpha, \beta, \ldots$ states to be eigenstates of the kinetic operator $K$, we have

$$K|m\rangle = E_m|m\rangle, \qquad K|\alpha\rangle = E_\alpha|\alpha\rangle, \qquad K|\beta\rangle = E_\beta|\beta\rangle, \qquad \ldots.$$

The Hubbard interaction $W$ can create or destroy up to two e–h pairs. Therefore, its action on an $m$ state yields

$$W|m\rangle = \sum_{m'} W_{m',m}|m'\rangle + \sum_\alpha W_{\alpha,m}|\alpha\rangle + \sum_\beta W_{\beta,m}|\beta\rangle,$$

that on an $\alpha$ states yields

$$W|\alpha\rangle = \sum_m W_{m,\alpha}|m\rangle + \sum_{\alpha'} W_{\alpha',\alpha}|\alpha'\rangle + \sum_\beta W_{\beta,\alpha}|\beta\rangle + \sum_\gamma W_{\gamma\alpha}|\gamma\rangle,$$

and so on. In this way we obtain an algebraic system for the coefficients of the configuration interaction of equation (12). In order to test the instability of the Fermi liquid towards pairing, it is sufficient to study the amplitudes $a_m$ of the $m$ states. In the weak-coupling limit this can be done by truncating the expansion (12) to the $\alpha$ states. As we have shown [48], the inclusion of the $\beta, \gamma, \ldots$ states produces a $E$-dependent renormalization of the matrix elements of higher order in $W$, leaving the structure of the equations unaltered.

By taking a linear combination of the $\alpha$ states in such a way that

$$(K+W)_{\alpha,\alpha'} = \delta_{\alpha\alpha'}E'_\alpha$$

the algebraic system reduces to

$$\begin{aligned} &[E_m - E]\, a_m + \sum_{m'} W_{m,m'}a_{m'} + \sum_\alpha W_{m,\alpha}a_\alpha = 0 \\ &\left[E'_\alpha - E\right] a_\alpha + \sum_{m'} W_{\alpha,m'}a_{m'} = 0. \end{aligned} \tag{13}$$

Solving for $a_\alpha$ and substituting back in equation (13), we end up with an equation for the dressed pair $|\psi\rangle \equiv \sum_m a_m|m\rangle$. The effective Schrödinger equation for the pair reads

$$(K + W + S[E])\,|\psi\rangle \equiv H_{\text{pair}}|\psi\rangle = E|\psi\rangle \tag{14}$$

where

$$(S[E])_{m,m'} = -\sum_\alpha \frac{W_{m,\alpha}W_{\alpha,m'}}{E'_\alpha - E} \tag{15}$$

is the scattering operator. The matrix elements $W_{m,m'}$ in equation (14) may be written as the sum of two terms representing the direct interaction $W^{(d)}_{m,m'}$ between the particles forming the pair and the first-order self-energy $W_m$:

$$W_{m,m'} = W^{(d)}_{m,m'} + \delta_{m,m'} W_m.$$

Similarly, in $S[E]$ we may recognize two different contributions; one is the true effective interaction $W_{\rm eff}$, while the other is the forward scattering term $F$

$$S_{m,m'} = (W_{\rm eff})_{m,m'} + F_m \delta_{m,m'}.$$

The first-order self-energy and the forward scattering term are diagonal in the indices $m$ and $m'$. $W_m$ and $F_m$ renormalize the non-interacting energy $E_m$ of the $m$ states:

$$E_m \to E^{(\rm R)}_m = E_m + W_m + F_m.$$

Equation (14) has the form of a Schrödinger equation with eigenvalue $E$ for the added pair with the interaction $W^{(d)} + W_{\rm eff}$. Here, the $W = 0$ pairs are special because $W^{(d)}$ vanishes. We interpret $a_m$ as the wavefunction of the dressed pair, which is acted upon by an effective Hamiltonian $H_{\rm pair}$. This way of looking at equation (14) is perfectly consistent, despite the presence of the many-body eigenvalue $E$. Indeed, if the interaction is attractive and produces bound states, the spectrum contains discrete states below the threshold of the continuum (two-electron Fermi energy). This is a clear-cut criterion for pairing, which is exact in principle. The threshold is given by

$$E^{(\rm R)}_{\rm F} \equiv \min_{\{m\}}[E^{(\rm R)}_m(E)],$$

and contains all the pairwise interactions except those between the particles in the pair. $E^{(\rm R)}_{\rm F}$ must be determined once equation (14) has been solved (since $F$ depends on the solution). The ground-state energy $E$ may be conveniently written as $E^{(\rm R)}_{\rm F} + \Delta$. $\Delta < 0$ indicates a Cooper-like instability of the normal Fermi liquid and its magnitude represents the binding energy of the pair.

It is worth noticing that in principle the canonical transformation is exact and it is not limited to the weak-coupling regime. In the numerical calculations, however, some approximation is needed. In practice, we shall compute the bare quantities; that is, we shall neglect the six-body and higher excitations in the calculation of $W_{\rm eff}$ and $F$. This is a reasonable approximation if we compute small corrections to a Fermi liquid background, and the exact numerical results obtained in small clusters suggest that this is the case; see the next section.

### *3.3. Pairing in the $CuO_4$ cluster*

We have defined the pairing energy for a cluster with $N+2$ particles by introducing the quantity $\tilde{\Delta}(N+2) = E(N+2) + E(N) - 2E(N+1)$. At weak coupling we have shown in [42] that $\tilde{\Delta}$ agrees with the binding energy $\Delta$ obtained from many-body perturbation theory. Here, we consider again the $CuO_4$ cluster; we intend to test our canonical transformation by comparing the analytic results with the exact diagonalization data obtained in section 2.

The $CuO_4$ cluster can host a $W = 0$ pair of $B_2$ symmetry. At weak coupling, we can ignore the effect of the renormalizations in equation (15). Furthermore, we can discard the inter-shell interactions. Indeed, the one-body levels of finite clusters are widely separated and the dominant contribution to the effective interaction comes from the intra-shell interaction. Accordingly, in equation (15) we set $m = m' = B_2$. The one-body levels and their symmetry labels are reported in table 2.

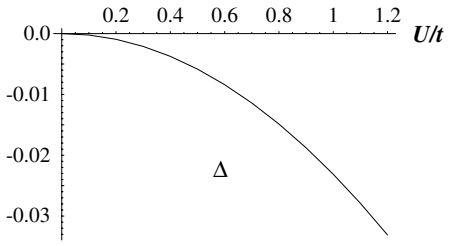


**Figure 5.** Trend of $\Delta$ versus $U/t$ in units of $t$.

The effective interaction in the $B_2$ symmetry channel is

$$W_{\rm eff}^{(B_2)} \equiv \sum_{\alpha} \frac{W_{B_2,\alpha} W_{\alpha,B_2}}{E_\alpha - E} = -\frac{U^2}{32}\left[\frac{2}{\varepsilon_{B_1} + \varepsilon_{A_1} - E} - \frac{1}{\varepsilon_{A_1'} + \varepsilon_{A_1} - E}\right].$$

The binding energy is obtained by expressing the lowest eigenvalue $E$ of $H_{\rm pair}$ as $E = E_{\rm F}^{(\rm R)} + \Delta$. The renormalized two-hole Fermi energy $E_{\rm F}^{(\rm R)}$ coincides with the bare one at this level of accuracy, i.e., $E_{\rm F}^{(\rm R)} = 2\varepsilon_{A_1}$. The results are shown in figure 5 for $\tau = 0$. We can see that $\Delta$ is negative and hence the renormalization approach predicts pairing, at least at weak coupling. We also observe that the order of magnitude of $|\Delta|$ is $10^{-2}t$, which is not comparable to any of the $U$ and $t$ input parameters. The reason is that the interaction, which vanishes identically for the *bare* $W = 0$ pairs, remains *dynamically* small for the dressed quasiparticles. This suggests that a *weak-coupling* theory may be useful to study the pairing force, despite the fact that $U$ is not small compared to $t$.

Next, we intend to compare $\Delta$ with the quantity $\tilde{\Delta}(4)$ obtained from exact diagonalizations; see figure 3. At weak coupling the agreement is excellent. However, $|\Delta|$ is $\sim$2 times greater than $|\tilde{\Delta}(4)|$ for $U/t \simeq 1$. This means that the inter-shell interactions and the renormalizations of the $\alpha$-state energies have an important weight in determining the right value of $\Delta$. However, what is comforting is that the analytic approach predicts the right trend of the binding energy. In the next section we shall use the canonical transformation to study larger and more physical systems.

### *3.4. Pairing in the $CuO_2$ plane: numerical results*

Using the analytic expression for the effective interaction in the full plane, we have performed exploratory numerical estimates of $\Delta$ by working on supercells of $N_\Lambda \times N_\Lambda$ cells, with periodic boundary conditions. For the sake of simplicity, we have neglected the minor contributions from the higher bands and considered the dominant intra-band processes, in which empty states belong to the bonding band. We have solved the problem in a virtually exact way for $N_\Lambda$ up to 40. Several supercell calculations have been reported to date [9], but no conclusive evidence of a pairing instability was reached due to the difficulty of dealing with size effects.

First, we have investigated triplet pairing but, as in the clusters, we have found a repulsive effective interaction. In contrast, $W = 0$ singlets show pairing, in line with our previous findings in small clusters [31, 40, 42]. Since screening excitations are explicitly accounted for in the Hamiltonian, it is likely that $U$ is a bare (unscreened) quantity, which justifies large values. A stronger interaction causes smaller pairs and speeds up convergence within attainable supercell sizes. In table 3, we report the results for ${}^1B_2$ pairs with $\varepsilon_{\rm F} = -1.3$ eV (half filling corresponds to $\varepsilon_{\rm F} = -1.384$ eV and we have used as input data the set of current parameters already used for clusters, that is (in eV) $t = 1.3$, $\varepsilon_{\rm p} = 3.5$, $\varepsilon_{\rm d} = 0$, $U_{\rm p} = 12.5$, $U_{\rm d} = 11.2$).

**Table 3.** Binding energy of $^1B_2$ pairs in supercells.

| $N_\Lambda$ | $\rho = N/N_\Lambda^2$ | $-\Delta$ (meV) | $V_{\rm eff}$ (eV) | $-\Delta_{\rm asympt}$ (meV) |
|---|---|---|---|---|
| 18 | 1.13 | 121.9 | 7.8 | 41.6 |
| 20 | 1.16 | 42.2 | 5.0 | 9.0 |
| 24 | 1.14 | 59.7 | 7.0 | 28.9 |
| 30 | 1.14 | 56.0 | 5.7 | 13.2 |
| 40 | 1.16 | 30.5 | 6.6 | 23.4 |

With supercell sizes $N_\Lambda > 40$ calculations become hard. Thus, we need a simple solvable model in supercells and in the infinite plane to make reliable extrapolations of numerical results. To this end, we introduce an average effective interaction (AEI) $-V_{\rm eff}$, $V_{\rm eff} > 0$, which is constant for all the empty states $\mathbf{k}$ and $\mathbf{k}'$. For any $N_\Lambda$, $V_{\rm eff}$ is implicitly defined from

$$\frac{8}{V_{\rm eff}} = \frac{1}{N_\Lambda^2} \sum_{\mathbf{k}} \frac{\theta(\varepsilon_{\mathbf{k}} - \varepsilon_{\rm F})}{2(\varepsilon_{\mathbf{k}} - \varepsilon_{\rm F}) + |\Delta|},$$

(the factor of eight comes from the projection onto the irrep $B_2$). Although $|\Delta|$ decreases monotonically with increasing $N_\Lambda$, $V_{\rm eff}$ remains fairly stable around 6–7 eV; see table 3. The relatively mild $N_\Lambda$ dependence of $V_{\rm eff}$ supports the use of the AEI to extrapolate the results to the thermodynamic limit. The asymptotic value $\lim_{N_\Lambda \to \infty} |\Delta| \equiv \Delta_{\rm asympt}$ can then be obtained from

$$\frac{8}{V_{\rm eff}} = \int_{\varepsilon_{\rm F}}^{0} \frac{{\rm d}\varepsilon \rho(\varepsilon)}{2(\varepsilon - \varepsilon_{\rm F}) + |\Delta_{\rm asympt}|},$$

where $\rho$ is the density of states.

The results for the $^1A_2$ pairs are seen to lead to bound states as well, with comparable $\Delta$ values [47]; the trend with doping is opposite, however, and the binding energy is nearly closing at $\varepsilon_{\rm F} = -1.1$ eV.

Although the three-band Hubbard model is an idealization of the strongly correlated $CuO_2$ planes, it is interesting to observe that evidence of mixed (s + id) symmetry for the pairing state has been amply reported in angle-resolved photoemission studies [50, 51].

## 4. The doped Hubbard antiferromagnet

The canonical transformation described in section 3.2 relies on the uniqueness of the non-interacting ground state $|\Phi_0(N)\rangle$. $|\Phi_0(N)\rangle$ is certainly unique if the Fermi surface is totally filled and it can be written as a Slater determinant. However, we are also particularly interested in the doped Hubbard antiferromagnet, and the antiferromagnetic ground state occurs at half filling, *not* in a filled-shell situation.

We want to study the doped antiferromagnet since there are strong indications that the Fermi liquid is unstable towards pairing near half filling; they come from diagrammatic approaches [15], renormalization group techniques [16, 17] and also cluster diagonalizations [30]. Therefore, exact results on the half-filled Hubbard model may be relevant to antiferromagnetism and to the mechanism of the superconducting instability as well. The Lieb theorem [23] on the ground-state spin degeneracy of the half-filled Hubbard model ensures that for any bipartite lattice $\Lambda = \mathcal{A} \cup \mathcal{B}$, with $|\mathcal{A}| = |\mathcal{B}|$, the ground state is unique for any interaction strength $U$. Thus, we can use the canonical transformation with $|\Phi_0(N)\rangle = \lim_{U \to 0^+} |\Phi_U(N)\rangle$ provided the number of holes $N$ equals the number of sites $|\Lambda|$. Remarkably, the $W = 0$ pairs are also essential tools to deal with the antiferromagnetic

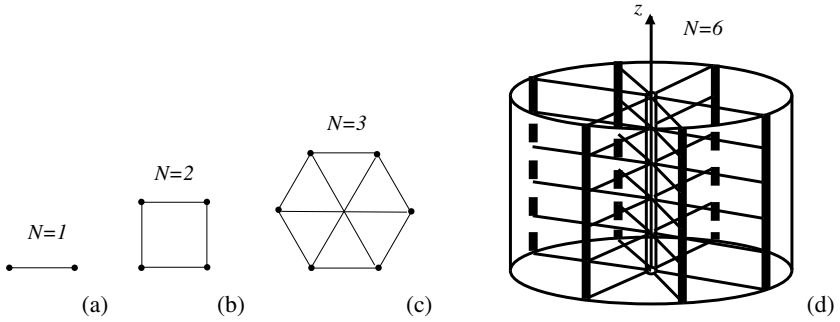


**Figure 6.** Physical representation of the CBG for $N = 1$ (a) and $N = 2$ (b) which is equivalent to a one-dimensional ring of length $L = 2, 4$ respectively. For $N = 3$ (c) we have the $(1, 1)$ nanotube of smallest length and periodic boundary conditions. For $N = 6$ (d) we present the gedanken device described in the text.

ground-state solution. Below, we present two exact results. First, we obtain the ground state $|\Phi_U(|\Lambda|)\rangle$ on the so called *complete bipartite graph* (CBG) for arbitrary but finite $U$. Then, we consider the square lattice and we resolve the degeneracy of the non-interacting ground-state multiplet at half filling. This latter result will then be used to study the pairing mechanism in the $4 \times 4$ Hubbard model.

### *4.1. Half-filled Hubbard model on the complete bipartite graph*

The complete bipartite graph (CBG) $\Lambda = \mathcal{A} \cup \mathcal{B}$ has bonds connecting any element of $\mathcal{A}$ with all the elements of $\mathcal{B}$. In figure 6 we have drawn a few examples of finite-size systems. For $N = 1$ and $N = 2$ the model is equivalent to a one-dimensional ring of length $L = 2, 4$ respectively. For $N = 3$ we have what can be understood as a prototype, $(1, 1)$ *nanotube* model, the one of smallest length $L = 1$, with periodic boundary conditions. For general $N$, one can conceive a gedanken device, like the one illustrated pictorially for $N = 6$ in figure 6(d). The $N$ vertical lines represent a realization of the $\mathcal{A}$ sublattice while the $\mathcal{B}$ sublattice is mimicked by the central object. The radial tracks in the figure represent conducting paths linking each $\mathcal{A}$ site to each $\mathcal{B}$ site according to the topology of our model.

Our solution is an example of an *antiferromagnetic* ground state in a model of itinerant electrons; it may provide useful hints about antiferromagnetism outside the strong-coupling regime (where the Hubbard model can be mapped onto the Heisenberg model).

The model is invariant under an arbitrary permutation of the $\mathcal{A}$ sites and/or of the $\mathcal{B}$ sites. In the symmetric case $|\mathcal{A}| = |\mathcal{B}|$ there is an additional $Z_2$ symmetry because of the $\mathcal{A} \leftrightarrow \mathcal{B}$ exchange. In what follows we shall focus on the symmetric case and we denote by $\mathcal{N}$ the number of sites in each sublattice, $|\Lambda| = 2\mathcal{N}$.

The one-body spectrum has three different eigenvalues $\varepsilon_g = -t$, $\varepsilon_0 = 0$, and $\varepsilon_{\bar{g}} = t$ with degeneracy $d_g = 1$, $d_0 = 2\mathcal{N} - 2$, and $d_{\bar{g}} = 1$ respectively. We use the convention $t > 0$ so that $\varepsilon_g$ is the lowest level and we shall denote by $\mathcal{S}_{hf}$ the set of zero-energy one-body eigenstates, $|\mathcal{S}_{hf}| = 2\mathcal{N} - 2$. The zero-energy one-body orbitals can be visualized by a simple argument. Consider any pair $i, j$, with $i \neq j$, of sites belonging to the same sublattice, say $\mathcal{A}$, and a wavefunction $\psi_{i,j}$ taking the values 1 and $-1$ on the pair and 0 elsewhere in $\mathcal{A}$ and in $\mathcal{B}$. It is evident that $\psi_{i,j}$ belongs to $\mathcal{S}_{hf}$. Operating on $\psi_{i,j}$ by the permutations of $S_{\mathcal{N}}$ we can generate a (non-orthogonal) basis of $\mathcal{N} - 1$ eigenfunctions vanishing in $\mathcal{B}$; further, by means

of the $Z_2$ symmetry, we obtain the remaining orbitals of $\mathcal{S}_{hf}$, which vanish on $\mathcal{A}$. This exercise shows that the group considered above justifies the $(2\mathcal{N}-2)$-fold degeneracy of the one-body spectrum.

We denote by $g$ ($\bar{g}$) the operator which annihilates a particle in the eigenstate with energy $\varepsilon_g$ ($\varepsilon_{\bar{g}}$). Then, the kinetic term $K$ can be written as

$$K = -t \sum_{\sigma} (g_\sigma^\dagger g_\sigma - \bar{g}_\sigma^\dagger \bar{g}_\sigma).$$

Next, we introduce the one-body eigenstate $a_i^\dagger|0\rangle$ of $\mathcal{S}_{hf}$ with vanishing amplitudes on the $\mathcal{B}$ sublattice. Similarly, $b_i^\dagger|0\rangle$ has vanishing amplitude on the $\mathcal{A}$ sublattice and therefore the $(2\mathcal{N}-2)$-body state

$$|\Phi_{\mathrm{AF}}^{(\sigma)}\rangle = a_{1\sigma}^\dagger \cdots a_{\mathcal{N}-1\sigma}^\dagger b_{1\bar{\sigma}}^\dagger \cdots b_{\mathcal{N}-1\bar{\sigma}}^\dagger |0\rangle, \qquad \bar{\sigma} = -\sigma \tag{16}$$

is an eigenstate of $K$ and of $W$ with vanishing eigenvalue. In the following we shall use the wording $W = 0$ *state* to denote any eigenstate of $H$ in the kernel of $W$. It is worth noticing that by mapping the $\mathcal{A}$ sites onto the $\mathcal{B}$ sites and vice versa, $|\Phi_{\mathrm{AF}}\rangle$ retains its form except for a spin flip; we call this property the *antiferromagnetic property* for obvious reasons.

The state $|\Phi_{\mathrm{AF}}\rangle$ plays a crucial role in building the exact ground state at half filling. We first observe that $|\Phi_{\mathrm{AF}}\rangle$ has non-vanishing projection onto all the total spin subspaces $S = 0, \ldots, \mathcal{N}-1$. Let us denote by $|\Phi_{\mathrm{AF}}^{0,0}\rangle$ the singlet component and by $|\Phi_{\mathrm{AF}}^{1,m}\rangle$, $m = 0, \pm 1$, the triplet component. We further introduce the short-hand notation $|g^0\rangle \equiv g_\uparrow^\dagger g_\downarrow^\dagger|0\rangle$ and $|\bar{g}^0\rangle \equiv \bar{g}_\uparrow^\dagger \bar{g}_\downarrow^\dagger|0\rangle$ for the two-body singlets that one obtains from the lowest- and the highest-energy orbitals $g$ and $\bar{g}$, and $|[g\bar{g}]^{1,m}\rangle$, $m = 0, \pm 1$, for the corresponding triplet. Then, one can prove [52] that the interacting ground state $|\Phi_U(|\Lambda|)\rangle$ can be written as

$$|\Phi_U(|\Lambda|)\rangle = \left[\gamma_g|g^0\rangle + \gamma_{\bar{g}}|\bar{g}^0\rangle\right] \otimes |\Phi_{\mathrm{AF}}^{0,0}\rangle + \gamma_0 \sum_{m=-1}^{1} (-)^m |[g\bar{g}]^{1,m}\rangle \otimes |\Phi_{\mathrm{AF}}^{1,-m}\rangle,$$

where $(\gamma_g, \gamma_{\bar{g}}, \gamma_0)$ is the lowest-energy eigenvector of a $3 \times 3$ Hermitian matrix [52].

We observe that $|\Phi_U(|\Lambda|)\rangle$ is an eigenstate of the total number operator $\hat{n}^a + \hat{n}^b$ of particles in the shell $\mathcal{S}_{hf}$, despite the fact that $[\hat{n}^a + \hat{n}^b, H] \neq 0$. Such a remarkable property (*shell population rigidity*) relies on the cancellation of those scattering amplitudes that do not preserve the number of particles in $\mathcal{S}_{hf}$. We have shown [52] that this cancellation takes place provided in $\mathcal{S}_{hf}$ the $(2\mathcal{N}-2)$-body state is a $W = 0$ state. We have also found that the ground-state energy $E(|\Lambda|)$ is negative for any value of the repulsion $U$; qualitatively, we may say that the particles manage to avoid the double occupation very effectively. Furthermore, $E(|\Lambda|)$ is a monotonically increasing function of $U$ and $\mathcal{N}$ due to the existence of non-trivial correlations even for large $\mathcal{N}$. The nature of these correlations has been investigated by computing the expectation value of the repulsion. We have shown that for any finite $\mathcal{N}$ there is a critical value of $U$ yielding maximum repulsion. Even more interesting is the magnetic order of the ground state. Due to the $S_\mathcal{N} \otimes S_\mathcal{N} \otimes Z_2$ symmetry, the spin–spin correlation function $G_{\mathrm{spin}}(i, j) \equiv \langle \Phi_U(|\Lambda|)|S_i^z S_j^z|\Phi_U(|\Lambda|)\rangle$ can be written as

$$G_{\mathrm{spin}}(i, j) = \begin{cases} G_0 & i = j \\ G_{\mathrm{on}} & i \in \mathcal{A}\,(i \in \mathcal{B}) \quad \text{and} \quad j \in \mathcal{A}\,(j \in \mathcal{B}) \\ G_{\mathrm{off}} & i \in \mathcal{A}\,(i \in \mathcal{B}) \quad \text{and} \quad j \in \mathcal{B}\,(j \in \mathcal{A}). \end{cases}$$

In figure 7 we report the trend of $G_{\mathrm{on}}$ and $G_{\mathrm{off}}$ versus $U$ for three different values of $\mathcal{N} = 2, 3, 10$. According to the Shen–Qiu–Tian theorem [53], $G_{\mathrm{on}}$ is always larger than zero

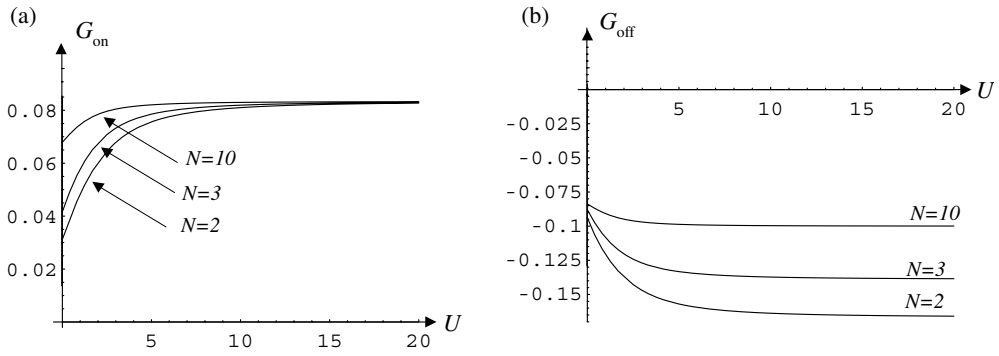


**Figure 7.** (a) $G_{\rm on}$ versus $U$ in the range $0 \leqslant U \leqslant 20$ for three different values of the number of sites $\mathcal{N} = 2, 3, 10$. (b) $G_{\rm off}$ versus $U$ in the range $0 \leqslant U \leqslant 20$ for three different values of the number of sites $\mathcal{N} = 2, 3, 10$. The hopping parameter has been chosen to be $t = 1$ in both cases.

while $G_{\rm off}$ is always negative. Next, we consider the ground-state average of the square of the staggered magnetization operator

$$m^2_{\rm AF} \equiv \frac{1}{|\Lambda|}\langle\Phi_U|\left[\sum_{i\in\Lambda}\epsilon(i)S^z_i\right]^2|\Phi_U\rangle, \qquad \epsilon(i) = 1, -1 \qquad \text{for } i \in \mathcal{A}, \mathcal{B}. \tag{17}$$

The Shen–Qiu–Tian theorem implies that each term in the expansion of equation (17) is non-negative. We emphasize, however, that for $|\mathcal{A}| = |\mathcal{B}|$ this does not imply that $m^2_{\rm AF}$ is an extensive quantity! Remarkably, in the CBG, $m^2_{\rm AF} = G_0 + (\mathcal{N}-1)G_{\rm on} - \mathcal{N}G_{\rm off}$ is extensive for any value of the on-site repulsion $U$ and provides the first example of an antiferromagnetic ground state in a model of itinerant electrons.

### *4.2. Half-filled Hubbard model on the square lattice for $U = 0^+$*

We consider the Hubbard Hamiltonian on the square lattice

$$H = K + W = \frac{t}{2}\sum_{\langle\mathbf{r},\mathbf{r}'\rangle\sigma}(c^\dagger_{\mathbf{r}\sigma}c_{\mathbf{r}'\sigma} + \text{h.c.}) + U\sum_{\mathbf{r}} n_{\mathbf{r}\uparrow}n_{\mathbf{r}\downarrow} \tag{18}$$

with $\mathbf{r} = (i_x, i_y)$, $i_x, i_y = 1, \ldots, N_\Lambda$ and the sum on $\langle\mathbf{r}, \mathbf{r}'\rangle$ over the pairs of nearest-neighbour sites. The point symmetry is $C_{4v}$; besides, $H$ is invariant under the commutative group of translations $\mathbf{T}$ and hence the space group $\mathbf{G} = \mathbf{T} \otimes C_{4v}$; $\otimes$ means the semidirect product. In terms of the Fourier expanded fermion operators (periodic boundary conditions) $c_{\mathbf{k}} = \frac{1}{N_\Lambda}\sum_{\mathbf{r}} \mathrm{e}^{\mathrm{i}\mathbf{k}\cdot\mathbf{r}}c_{\mathbf{r}}$, we have $K = \sum_{\mathbf{k}} \varepsilon_{\mathbf{k}} c^\dagger_{\mathbf{k}\sigma}c_{\mathbf{k}\sigma}$ with $\varepsilon_{\mathbf{k}} = 2t[\cos k_x + \cos k_y]$. Then, the one-body plane-wave state $c^\dagger_{\mathbf{k}\sigma}|0\rangle \equiv |\mathbf{k}\sigma\rangle$ is an eigenstate of $K$.

In this section we build the exact ground state of the Hubbard Hamiltonian (18) at half filling and weak coupling for a general *even* $N_\Lambda$. Once a unique non-interacting ground state is determined, one can use the non-perturbative canonical transformation to test the instability of the system towards pairing; this will be done in the next section for $N_\Lambda = 4$.

The starting point is the following property of the number operator: $n_{\mathbf{r}} = c^\dagger_{\mathbf{r}}c_{\mathbf{r}}$ (for the moment we omit the spin index).

**Theorem.** *Let $\mathcal{S}$ be an arbitrary set of plane-wave eigenstates $\{|\mathbf{k}_i\rangle\}$ of $K$ and $(n_{\mathbf{r}})_{ij} = \langle\mathbf{k}_i|n_{\mathbf{r}}|\mathbf{k}_j\rangle = \frac{1}{N^2_\Lambda}\mathrm{e}^{\mathrm{i}(\mathbf{k}_i-\mathbf{k}_j)\cdot\mathbf{r}}$ the matrix of $n_{\mathbf{r}}$ in $\mathcal{S}$. This matrix has eigenvalues $\lambda_1 = \frac{|\mathcal{S}|}{N^2_\Lambda}$ and $\lambda_2 = \cdots = \lambda_{|\mathcal{S}|} = 0$.*

Note that $|\mathcal{S}| \leqslant N_\Lambda^2$; if $|\mathcal{S}| = N_\Lambda^2$ the set is complete, like the set of all orbitals, and the theorem is trivial (a particle on site $\mathbf{r}$ is the $n_\mathbf{r}$ eigenstate with unit eigenvalue). Otherwise, if $|\mathcal{S}| < N_\Lambda^2$, the theorem is an immediate consequence of the fact [55] that

$$\det|(n_\mathbf{r})_{ij} - \lambda\delta_{ij}| = (-\lambda)^{|\mathcal{S}|-1}\left(\frac{|\mathcal{S}|}{N_\Lambda^2} - \lambda\right), \qquad \forall \mathbf{r}. \tag{19}$$

Let $\mathcal{S}_{hf}$ denote the set (or shell) of the $\mathbf{k}$ wavevectors such that $\varepsilon_\mathbf{k} = 0$. At half filling ($N_\Lambda^2$ particles) for $U = 0$ the $\mathcal{S}_{hf}$ shell is half occupied, while all $\mathbf{k}$ orbitals such that $\varepsilon_\mathbf{k} < 0$ are filled. The $\mathbf{k}$ vectors of $\mathcal{S}_{hf}$ lie on the square having vertices $(\pm\pi, 0)$ and $(0, \pm\pi)$; one readily realizes that the dimension of the set $\mathcal{S}_{hf}$ is $|\mathcal{S}_{hf}| = 2N_\Lambda - 2$. Since $N_\Lambda$ is even and $H$ commutes with the total spin operators, at half filling every ground state of $K$ is represented in the $S^z = 0$ subspace. Thus, $K$ has $\binom{2N_\Lambda - 2}{N_\Lambda - 1}^2$ degenerate unperturbed ground-state configurations with $S^z = 0$. Most of the degeneracy is removed in first order by $W$. We shall be able to single out the unique ground state of $H$ by exploiting the Lieb theorem.

The first-order splitting of the degeneracy is obtained by diagonalizing the $W$ matrix over the unperturbed basis; as in elementary atomic physics, the filled shells just produce a constant shift of all the eigenvalues and henceforth may be ignored in first-order calculations. In other terms we consider the *truncated Hilbert space* $\mathcal{H}$ spanned by the *states of* $N_\Lambda - 1$ *holes of each spin in* $\mathcal{S}_{hf}$, and we want the *exact* ground state(s) of $W$ in $\mathcal{H}$; by construction $\mathcal{H}$ is in the kernel of $K$, so the ground state of $W$ is the ground state of $H$ as well. Since the lowest eigenvalue of $W$ is zero, it is evident that any $W = 0$ state in $\mathcal{H}$ is a ground state of $H$.

To diagonalize the *local* operator $W$ in closed form we need to set up a *local* basis set of one-body states. If $\mathcal{S}_{hf}$ were the complete set of plane-wave states $\mathbf{k}$, the new basis would be trivially obtained by a Fourier transformation, but this is not the case. We introduce a set $\{|\varphi_\alpha^{(\mathbf{r})}\rangle\}$ of orbitals such that $n_\mathbf{r}$ is diagonal in this basis. The eigenvectors $|\varphi_\alpha^{(0)}\rangle$ of $n_{\mathbf{r}=0}$ and those $|\varphi_\alpha^{(\mathbf{r})}\rangle$ of other sites $\mathbf{r}$ are connected by translation and also by a unitary transformation, or change of basis set. Picking $\mathbf{r} = \hat{e}_l$, $l = x$ means $\hat{e}_l = (1, 0)$ or transfer by one step towards the right and $l = y$ means $\hat{e}_l = (0, 1)$ or transfer by one step upwards. The unitary transformation reads

$$|\varphi_\alpha^{(\hat{e}_l)}\rangle = \sum_{\beta=1}^{2N_\Lambda-2} |\varphi_\beta^{(0)}\rangle\langle\varphi_\beta^{(0)}|\varphi_\alpha^{(\hat{e}_l)}\rangle \equiv \sum_{\beta=1}^{2N_\Lambda-2} |\varphi_\beta^{(0)}\rangle T_{l_{\beta\alpha}}. \tag{20}$$

The transfer matrix $T_l$ *knows* all the translational and point symmetry of the system, and will turn out to be very special.

For large $N_\Lambda$, to find $\{|\varphi_\alpha^{(\mathbf{r})}\rangle\}$ it is convenient to separate the $\mathbf{k}$ of $\mathcal{S}_{hf}$ in irreducible representations of the space group $\mathbf{G} = C_{4v} \otimes \mathbf{T}$. Choosing an arbitrary $\mathbf{k} \in \mathcal{S}_{hf}$ with $k_x \geqslant k_y \geqslant 0$, the set of vectors $R_i\mathbf{k}$, where $R_i \in C_{4v}$, is a (translationally invariant) basis for an irrep of $\mathbf{G}$. The high-symmetry vectors $(0, \pi)$ and $(\pi, 0)$ always transform among themselves and are the basis of the only two-dimensional irrep of $\mathbf{G}$, which exists for any $N_\Lambda$. If $N_\Lambda/2$ is even, one also finds the high-symmetry wavevectors $\mathbf{k} = (\pm\pi/2, \pm\pi/2)$ which mix among themselves and yield a four-dimensional irrep. In general, the vectors $R_i\mathbf{k}$ are all different, so all the other irreps of $\mathbf{G}$ have dimension eight, the number of operations of the point group $C_{4v}$.

Next, we show how to build our *local* basis set and derive $W = 0$ states for each kind of irrep of $\mathbf{G}$. For illustration, we shall first consider the case $N_\Lambda = 4$; then $\mathcal{S}_{hf}$ contains the bases of two irreps of $\mathbf{G}$, of dimensions two and four. The one with basis $\mathbf{k}_A = (\pi, 0)$, $\mathbf{k}_B = (0, \pi)$ breaks into $A_1 \oplus B_1$ in $C_{4v}$.

The eigenstates of $(n_{\mathbf{r}=0})_{ij} = \langle\mathbf{k}_i|n_{\mathbf{r}=0}|\mathbf{k}_j\rangle$, with $i, j = A, B$, are $|\psi''_{A_1}\rangle = \frac{1}{\sqrt{2}}(|\mathbf{k}_A\rangle + |\mathbf{k}_B\rangle)$ with $\lambda_1 = 1/8$ and $|\psi''_{B_1}\rangle = \frac{1}{\sqrt{2}}(|\mathbf{k}_A\rangle - |\mathbf{k}_B\rangle)$ with $\lambda_2 = 0$. Since under translation by

a lattice step $T_l$ along the $l = x, y$ direction $|\mathbf{k}\rangle \rightarrow \mathrm{e}^{\mathrm{i}k_l}|\mathbf{k}\rangle$, using equation (20) one finds that $|\psi''_{A_1}\rangle \leftrightarrow (-1)^{\theta''_l}|\psi''_{B_1}\rangle$, with $\theta''_x = 1, \theta''_y = 0$; so $|\psi''_{A_1}\rangle$ has vanishing amplitude on one sublattice and $|\psi''_{B_1}\rangle$ on the other. The two-body state $|\psi''_{A_1}\rangle_\sigma|\psi''_{B_1}\rangle_{-\sigma}$ has occupation for spin $\sigma$ but not for spin $-\sigma$ on the site $\mathbf{r} = 0$; under a lattice step translation it flips the spin and picks up a $(-1)$ phase factor: $|\psi''_{A_1}\rangle_\sigma|\psi''_{B_1}\rangle_{-\sigma} \leftrightarrow |\psi''_{B_1}\rangle_\sigma|\psi''_{A_1}\rangle_{-\sigma}$; therefore, it has double occupation nowhere and is a $W = 0$ state ($W = 0$ pair [47, 48]).

The four-dimensional irrep with basis $\mathbf{k}_1 = (\pi/2, \pi/2)$, $\mathbf{k}_2 = (-\pi/2, \pi/2)$, $\mathbf{k}_3 = (\pi/2, -\pi/2)$ $\mathbf{k}_4 = (-\pi/2, -\pi/2)$ breaks into $A_1 \oplus B_2 \oplus E$ in $C_{4v}$; letting $I = 1, 2, 3, 4$ for the irreps $A_1$, $B_2$, $E_x$, $E_y$ respectively, we can write down all the eigenvectors of $(n_{\mathbf{r}=0})_{ij} = \langle \mathbf{k}_i|n_{\mathbf{r}=0}|\mathbf{k}_j\rangle$, with $i, j = 1, \ldots, 4$, as $|\psi'_I\rangle = \sum_{i=1}^4 O'_{Ii}|\mathbf{k}_i\rangle$, where $O'$ is a $4 \times 4$ orthogonal matrix. The state with non-vanishing eigenvalue is again the $A_1$ eigenstate. After a little bit of algebra we have shown [55] that under $T_l$ the subspace of $A_1$ and $B_2$ symmetry is exchanged with that of $E_x$ and $E_y$ symmetry. Thus we can build a four-body eigenstate of $W$ with vanishing eigenvalue: $|\psi'_{A_1}\psi'_{B_2}\rangle_\sigma|\psi'_{E_x}\psi'_{E_y}\rangle_{-\sigma}$. As before under a lattice step translation this state does not change its spatial distribution but $\sigma \rightarrow -\sigma$ without any phase factor: $|\psi'_{A_1}\psi'_{B_2}\rangle_\sigma|\psi'_{E_x}\psi'_{E_y}\rangle_{-\sigma} \leftrightarrow |\psi'_{E_x}\psi'_{E_y}\rangle_\sigma|\psi'_{A_1}\psi'_{B_2}\rangle_{-\sigma}$.

Now we use these results to diagonalize $n_{\mathbf{r}=0}$ on the whole set $\mathcal{S}_{hf}$ (we could have done that directly by diagonalizing $6 \times 6$ matrices but we wanted to show the general method). The eigenstate of $n_{\mathbf{r}=0}$ with non-vanishing eigenvalue always belongs to $A_1$. The matrix $n_{\mathbf{r}}$ has eigenvalues three-eighths and (five times) zero, as predicted by equation (19). For $\mathbf{r} = 0$ the eigenvector of occupation three-eighths is $|\varphi_1^{(0)}\rangle = \frac{1}{\sqrt{3}}|\psi''_{A_1}\rangle + \sqrt{\frac{2}{3}}|\psi'_{A_1}\rangle$. The other $A_1$ eigenstate of $n_{\mathbf{r}=0}$ has zero eigenvalue and reads $|\varphi_2^{(0)}\rangle = \sqrt{\frac{2}{3}}|\psi''_{A_1}\rangle - \frac{1}{\sqrt{3}}|\psi'_{A_1}\rangle$. The other eigenvectors, whose symmetry differs from $A_1$, are $|\varphi_3^{(0)}\rangle = |\psi'_{B_2}\rangle$, $|\varphi_4^{(0)}\rangle = |\psi''_{B_1}\rangle$, $|\varphi_5^{(0)}\rangle = |\psi'_{E_x}\rangle$ and $|\varphi_6^{(0)}\rangle = |\psi'_{E_y}\rangle$. One finds [55] that the transfer matrices $T_l$ of equation (20) such that $|\varphi_I^{(\hat{e}_l)}\rangle \equiv \sum_J |\varphi_J^{(0)}\rangle T_{l_{JI}}$ are *antiblock diagonal*. Thus, the local basis at any site $\mathbf{r}$ splits into the subsets $\mathcal{S}_a = \{|\varphi_1^{(0)}\rangle, |\varphi_2^{(0)}\rangle, |\varphi_3^{(0)}\rangle\}$, and $\mathcal{S}_b = \{|\varphi_4^{(0)}\rangle, |\varphi_5^{(0)}\rangle, |\varphi_6^{(0)}\rangle\}$; a shift by a lattice step sends members of $\mathcal{S}_a$ into linear combinations of the members of $\mathcal{S}_b$, and conversely.

Consider the six-body eigenstate of $K$

$$|\Phi_{\mathrm{AF}}\rangle_\sigma = |\varphi_1^{(0)}\varphi_2^{(0)}\varphi_3^{(0)}\rangle_\sigma|\varphi_4^{(0)}\varphi_5^{(0)}\varphi_6^{(0)}\rangle_{-\sigma}.$$

In this state there is partial occupation of site $\mathbf{r} = 0$ with spin $\sigma$, but no double occupation. It turns out that a shift by a lattice step produces the transformation

$$|\Phi_{\mathrm{AF}}\rangle_\sigma \longleftrightarrow -|\Phi_{\mathrm{AF}}\rangle_{-\sigma}$$

that is, a lattice step is equivalent to a spin flip, a feature that we have already met in section 4.1 (*antiferromagnetic property*). Since the spin-flipped state is also free of double occupation, $|\Phi_{\mathrm{AF}}\rangle_\sigma$ is a $W = 0$ eigenstate. A ground state which is a single determinant is quite an unusual property for an interacting model like this.

Note that $|\varphi_1^{(0)}\varphi_2^{(0)}\rangle$ is equivalent to $|\psi''_{A_1}\psi'_{A_1}\rangle$, because this is just a unitary transformation of the $A_1$ wavefunctions; so $|\Phi_{\mathrm{AF}}\rangle_\sigma$ can also be written in terms of the old local orbitals (without any mix of the local states of different irreps of $\mathbf{G}$):

$$|\Phi_{\mathrm{AF}}\rangle_\sigma = |\psi''_{A_1}\psi'_{A_1}\psi'_{B_2}\rangle_\sigma|\psi''_{B_1}\psi'_{E_x}\psi'_{E_y}\rangle_{-\sigma}. \tag{21}$$

This form of the ground state lends itself to be generalized to arbitrary even $N_\Lambda$; see [54, 55].

A few further remarks about $|\Phi_{\mathrm{AF}}\rangle_\sigma$ are in order.

(1) Introducing the projection operator $P_S$ on the spin $S$ subspace, one finds that $P_S|\Phi_{\mathrm{AF}}\rangle_\sigma \equiv |\Phi^S_{\mathrm{AF}}\rangle_\sigma \neq 0$, $\forall S = 0, \ldots, N_\Lambda - 1$. Then, ${}_\sigma\langle\Phi_{\mathrm{AF}}|W|\Phi_{\mathrm{AF}}\rangle_\sigma = \sum_{S=1}^{N_\Lambda - 1} {}_\sigma\langle\Phi^S_{\mathrm{AF}}|W$

**Table 4.** One-body spectrum of the $4 \times 4$ Hubbard model for $t = -1$. We have used the notation introduced in [59] in labelling the irreducible representations.

| Energy | Irrep of $\mathcal{G}$ | Degeneracy |
|---|---|---|
| 4 | $\tilde{B}_2$ | 1 |
| 2 | $\Lambda_4$ | 4 |
| 0 | $\Omega_4$ | 6 |
| $-2$ | $\Lambda_1$ | 4 |
| $-4$ | $A_1$ | 1 |

$|\Phi^S_{\rm AF}\rangle_\sigma = 0$, and this implies that there is at least one ground state of $W$ in $\mathcal{H}$ for each $S$. The actual ground state of $H$ at weak coupling is the singlet $|\Phi^0_{\rm AF}\rangle_\sigma$.

(2) The *existence* of this singlet $W = 0$ ground state is a direct consequence of the Lieb theorem [23]. Indeed the maximum spin state $|\Phi^{N_\Lambda - 1}_{\rm AF}\rangle_\sigma$ is trivially in the kernel of $W$; since the ground state must be a singlet it should be an eigenvector of $W$ with vanishing eigenvalue.

(3) The above results and Lieb's theorem imply that higher-order effects split the ground-state multiplet of $H$ and the singlet is lowest.

(4) The Lieb theorem makes no assumptions concerning the lattice structure; adding the ingredient of the **G** symmetry we are able to explicitly display the wavefunction at weak coupling.

Using the explicit form of $P_{S=0}$ one finds that $P_{S=0}|\Phi_{\rm AF}\rangle_\sigma = -P_{S=0}|\Phi_{\rm AF}\rangle_{-\sigma}$. This identity allows us to study how the singlet component transforms under translations, reflections and rotations. In particular the *antiferromagnetic property* tells us that the total momentum is $K_{\rm tot} = (0, 0)$. To make contact with [56] we have also determined how $|\Phi^0_{\rm AF}\rangle$ transforms under the $C_{4v}$ operations with respect to the centre of an arbitrary plaquette. It turns out [55] that it is even under reflections and transforms as an s wave if $N_\Lambda/2$ is even and as a d wave if $N_\Lambda/2$ is odd.

In the next section we use these results, togheter with the non-perturbative canonical transformation, to study the doped $4 \times 4$ lattice at half filling. Since the non-interacting ground state at half filling is now well known and unambiguously defined, the expansion (12) can be performed in a unique way.

### *4.3. Pairing in the doped Hubbard antiferromagnet*

The one-body spectrum of the $4 \times 4$ Hubbard model has five equally spaced levels; see table 4. The space group **G** (containing the translations and the eight $C_{4v}$ operations) cannot explain the degeneracy of six, since in the $4 \times 4$ lattice the largest dimension of the irreps is four. As observed by previous authors [57, 58], the $4 \times 4$ lattice can be mapped into the $2 \times 2 \times 2 \times 2$ hypercube since each pair of next-nearest-neighbour sites has two nearest-neighbour sites in common. This implies that $H$ is invariant under a new and largest symmetry group; let us call it $\mathcal{G}$.

Due to the importance of the symmetry in our configuration interaction mechanism, we have explicitly calculated the character table of $\mathcal{G}$ taking into account an extra non-isometric symmetry operation [59]. $\mathcal{G}$ has 384 elements, 20 classes and hence 20 irreps whose dimensionality fully justifies the degeneracies of table 4.

As observed in section 4.1 the canonical transformation applies when two holes are added to a non-degenerate vacuum. To study the system at and close to half filling, we have to use

the results of section 4.2. In the following we will solve the problem of two electrons added to the half-filled system.

*4.3.1. $W = 0$ pairs.* In order to study the $W = 0$ pairing in the doped $4 \times 4$ antiferromagnet, we consider $W = 0$ pairs in the sixfold degenerate one-body level (belonging to $\Omega_4$). Exploiting the $W = 0$ theorem, we have found [59] $W = 0$ pairs with symmetry $\Gamma_1$, $\Gamma_2$, $\Sigma_2$, $\Omega_1$ and triplet pairs with symmetry $\Sigma_3$, $\Omega_2$, $\Omega_3$. Here, we are using the notation of [59]; the irreps $\Omega$ have dimension six, the $\Sigma$ have dimension three, and the $\Gamma$ have dimension two.

Exact diagonalization results [30] show that for $U/t < 3$ and $16 - 2 = 14$ holes the ground state is sixfold degenerate. Below, we use the canonical transformation and prove that the ground state corresponds to an $\Omega_1$ $W = 0$ *electron* pair over the half-filled system. For $U/t > 3$ and the same number of holes a level crossing takes place: the ground state is threefold degenerate and contains a state with momentum $(0, 0)$ and a doublet with momentum $(\pi, 0)$ and $(0, \pi)$. Again, the computed ground state can be assigned to a $\Sigma_2$ *electron* pair over the half-filled system [59].

*4.3.2. Pairing mechanism.* We consider the ground state of the $4 \times 4$ Hubbard model with 14 holes; aside from the 10 holes in the inner $A_1$ and $\Lambda_1$ shells (see table 4), the outer $\Omega_4$ shell contains four holes. We intend to show how pairing between two *electrons* added to the antiferromagnetic 16-hole ground state (half filling) comes out. We use the antiferromagnetic ground state $|\Phi_{\mathrm{AF}}^{S=0}\rangle$ as the non-interacting ground state of the configuration interaction expansion (12). With respect to this *electron vacuum*, the $m$ states are now $W = 0$ pairs of *electrons* added to $|\Phi_{\mathrm{AF}}^{S=0}\rangle$. In the $4 \times 4$ lattice the one-body energy levels are widely separated and the dominant interaction is between electrons in the same shell. Therefore, we consider as $m$ states only the $W = 0$ electron pairs in the shell $\mathcal{S}_{hf}$, i.e., those belonging to the irreps $\Omega_1$ and $\Sigma_2$, and we neglect the high-lying unoccupied orbitals. Explicit calculations [59] show that the effective interaction is attractive for both $\Omega_1$ and $\Sigma_2 W = 0$ electron pairs and that the corresponding binding energy is $\Delta_{\Omega_1} = -61.9$ meV and $\Delta_{\Sigma_2} = -60.7$ meV for $U = -t = 1$ eV. Therefore, the weak-coupling ground state can be interpreted as an $\Omega_1$ $W = 0$ electron pair over the antiferromagnetic ground state. This result agrees with exact diagonalization data [30].

## 5. Carbon nanotubes and triangular cobalt oxides

### *5.1. Nanotubes*

There is experimental evidence that the critical temperature $T_c$ in alkali–graphite intercalation compounds $C_xM$ (where M is a given alkali metal) grows as $x$ decreases [60]. Under high pressure, high-metal-concentration samples such as $C_6K$, $C_3K$, $C_4Na$, $C_3Na$, $C_2Na$, and $C_2Li$ have been synthesized; for $C_2Na$ the value of $T_c$ is 5 K while for $C_2Li$ $T_c = 1.9$ K. Recently, potassium [61] and lithium [62] have also been intercalated in ropes of single- and multi-wall carbon nanotubes (the highest metal concentration was obtained with lithium in $C_2Li$), and a net charge transfer between the alkali metals and the carbon atoms has been predicted [63]. The alkali metals cause little structural deformation, but increase the filling of the original bands. Nanotubes close to half filling are deemed to be Luttinger liquids down to millikelvin temperatures [64, 65]. Here [66], we use the Hubbard Hamiltonian $H$ on the wrapped honeycomb lattice to represent the valence bands of single-wall carbon nanotubes (SWNTs) and we apply our symmetry-driven configuration interaction pairing mechanism based on the existence of $W = 0$ pairs. We shall focus on armchair $(N, N)$ SWNTs and show that the

pair binding energy grows as the number of electrons per C atom increases. Furthermore, a stronger binding in nanotubes than in graphite sheets is predicted, which suggests a higher critical temperature in the former. This is also supported by the measurements of a $T_c \approx 15$ K in 4 Å SWNTs by Tang *et al* [3].

Any armchair SWNT has a bonding (−) and an antibonding (+) band, and the Fermi line has $C_{2v}$ symmetry ($C_{6v}$ is the symmetry group of the graphite sheet). Since these systems are usually doped with *electrons*, we take the Fermi level $\varepsilon_F$ to lie in the antibonding band. We use the $W = 0$ theorem for electrons with opposite quasimomentum and we find $W = 0$ pairs belonging to the pseudoscalar irrep $A_2$ of $C_{2v}$. Let $(a, b)$ denote the basis of the Bravais lattice and $u(\mathbf{k}, \zeta)$ the periodic part of the Bloch function of quasi-momentum $\mathbf{k}$, with $\zeta = a, b$. The singlet pair wavefunction reads [66]

$$\psi^{[A_2]}_{\zeta_1,\zeta_2}(\mathbf{k}, \mathbf{R}_1, \mathbf{R}_2) = \frac{1}{\sqrt{2}} \sin(k_x(X_1 - X_2)) \times \left[u^*(\mathbf{k}, \zeta_1)\, u^*(-\mathbf{k}, \zeta_2)\, e^{ik_y(Y_1-Y_2)} - u^*(\mathbf{k}, \zeta_2)\, u^*(-\mathbf{k}, \zeta_1)\, e^{-ik_y(Y_1-Y_2)}\right],$$

with $\mathbf{R}_i = (X_i, Y_i)$ the origin of the cell where the particle $i$ lies. We can verify by direct inspection that the $W = 0$ pair wavefunction $\psi^{[A_2]}$ vanishes for $X_1 = X_2$, that is if the particles lie on the same annulus of the armchair tube.

The effective interaction $W_{\text{eff}}$ between the particles of a $W = 0$ pair can be obtained analytically by the canonical transformation approach described in section 3.2. We let $\varepsilon(\mathbf{k})$ be the one-body energy excitation with momentum $\mathbf{k}$ in the antibonding band and we call $\mathcal{D}/4$ a quarter of the empty part of the FBZ. The effective Schrödinger equation for the pair reads

$$[2\varepsilon(\mathbf{k}) + W_F + F(\mathbf{k}, E)]\, a_{\mathbf{k}} + \sum_{\mathbf{k}' \in \mathcal{D}/4} W_{\text{eff}}(\mathbf{k}, \mathbf{k}', E) a_{\mathbf{k}'} = E a_{\mathbf{k}}, \tag{22}$$

where $W_F$ is the first-order self-energy shift (which we found to be independent of $\mathbf{k}$) and $F(\mathbf{k}, E)$ is the forward scattering term (which does not contains any direct interaction between the particles of the pair). Equation (22) requires a self-consistent calculation of $E$ (since $W_{\text{eff}}$ and $F$ are $E$ dependent). We show below that $E = 2\varepsilon_F + W_F + F_{\min}(\mathbf{k}_F) + \Delta$, with a positive binding energy $-\Delta$ of the $W = 0$ pair; here, $F_{\min}(\mathbf{k}_F)$ is the minimum value of $F(\mathbf{k}, E)$ among the $\mathbf{k}_F$-wavevectors on the Fermi line.

First, we obtained a direct verification that pairing actually occurs in the (1, 1) nanotube of length $L = 2$ (in units of the lattice spacing) and periodic boundary conditions. As for the $CuO_4$, we compute the quantity $\tilde{\Delta}(4) = E(4) + E(2) - 2E(3)$ and we compare it with $\Delta$ (obtained from the canonical transformation). $\tilde{\Delta}(4)$ has been computed in a large range of $U/t$ values, and its trend is shown in figure 8(a). In figure 8(b) we report the comparison between $\tilde{\Delta}(4)$ and $\Delta$. We observe that the analytical value $|\Delta|$ is about twice $|\tilde{\Delta}(4)|$ for $U/t \simeq 1$, as for the $CuO_4$ cluster. However, the analytical approach predicts the right trend of the binding energy and it is very reliable in the weak-coupling regime.

Next, we consider supercells of $2N \times L = N_C$ cells, where $L$ is the length of the $(N, N)$ nanotube in units of the lattice spacing. We solve the Cooper-like equation (22) in a virtually exact way for $N$ up to 6 and $L$ up to 25, using $U/t = 2.5$ (which is of the correct order of magnitude for graphite [67, 68]). The canonical transformation overestimates $\Delta$ in this range of $U/t$, but remains qualitatively correct. The calculations are performed with the Fermi energy $\varepsilon_F$ varying between $0.8t$ and $1.1t$ (half filling corresponds to $\varepsilon_F = 0$). As in the (1, 1) nanotube, the $W = 0$ pairs are bound once dressed by the electron–hole excitations. However, the binding energy $-\Delta$ decreases monotonically both with the radius and the length of the tube.

With supercell sizes $N_C > 300$ numerical calculations become hard and the AEI scheme is used in order to get reliable extrapolations. The AEI $V_{\text{eff}}$ remains fairly stable around $\approx$1.5–2$t$

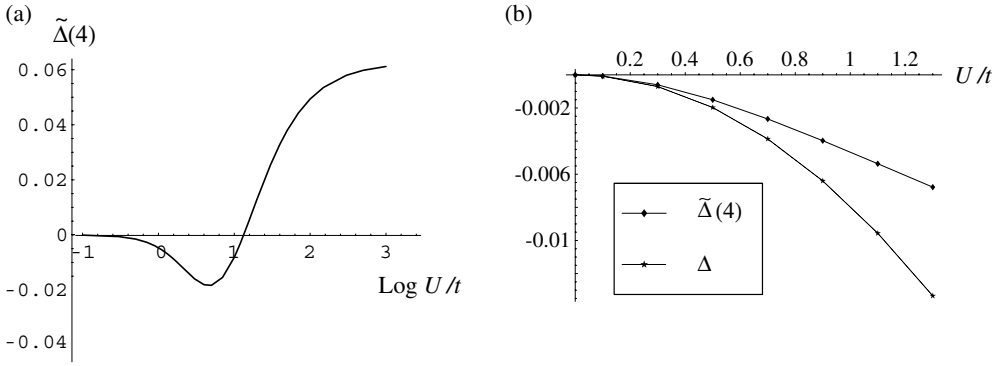


**Figure 8.** (a) Trend of $\tilde{\Delta}(4)$ in units of $t$ versus $\log U/t$ in the range $-1$ to 3 for the (1, 1) nanotube. (b) Comparison between $\Delta$ and $\tilde{\Delta}(4)$.

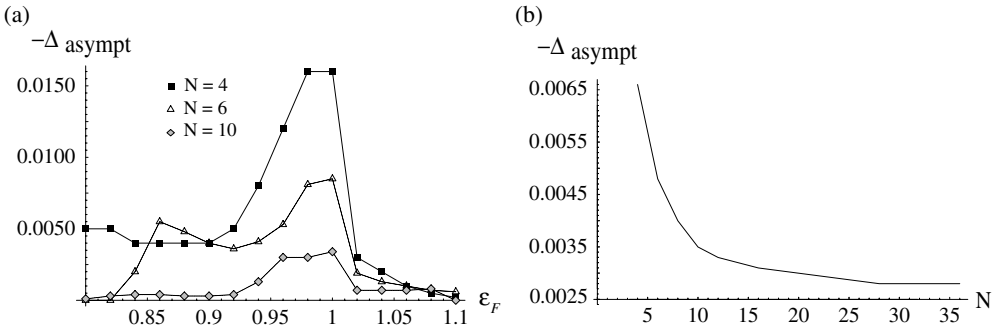


**Figure 9.** (a) Results of the canonical transformation approach with $U/t = 2.5$. $-\Delta_{\text{asympt}}$ as a function of the Fermi energy $\varepsilon_{\text{F}}$ for $N = 4$ (black boxes), $N = 6$ (empty triangles) and $N = 10$ (grey diamonds). The Fermi energy varies in the range 0.8–1.1$t$. (b) $-\Delta_{\text{asympt}}$ as a function of $N$ for $N$ in the range 6–36 with $\varepsilon_{\text{F}} = t$ and average effective interaction $V = 1.5t$. In both figures $-\Delta_{\text{asympt}}$ is in units of $t$.

for $N > 2$ with increasing $L$. Furthermore, $V_{\text{eff}}$ is largely independent of the Fermi energy. The weak dependence of $V_{\text{eff}}$ on the length $L$ allows for extrapolating the asymptotic value of the binding energy $\Delta_{\text{asympt}}(N) = \lim_{L\to\infty} \Delta(N, L)$, see also section 3.4. The results are shown in figure 9(a) with $V_{\text{eff}} = 1.5t$. We found that $\Delta_{\text{asympt}}$ is strongly dependent on the filling at fixed $N$; the sharp maximum at the *optimal doping* $\varepsilon_{\text{F}} \approx t$ (which corresponds to a number of electrons per graphite atom of 1.25) can be understood in terms of a corresponding peak in the density of states. In the *optimally doped* case $-\Delta_{\text{asympt}}(N)$ decreases monotonically as the radius of the tube increases; see figure 9(b). The decreasing of the binding energy with $N$ is suggested by recent measurements on nanotubes with diameter of few ångströms [3]. However, in the limit of large $N$, $\Delta_{\text{asympt}}(N)$ remains stable around $0.0028t$ and may be interpreted as the binding energy of the $W = 0$ pair in an *optimally doped* graphite sheet.

We emphasize that our pairing mechanism uses degenerate electronic states that exist in 2D (or quasi-2D) and works away from half filling. A proper account for the transverse direction is crucial in order to have a non-Abelian symmetry group and hence $W = 0$ pairs. The $\psi^{[A_2]}$ pair wavefunction vanishes when the transverse component $k_y = 0$. This opens up the interesting possibility that in nanotubes two distinct superconducting order parameters appear in the phase diagram, if it turns out that close to half-filling there is another one which breaks down the Luttinger liquid.

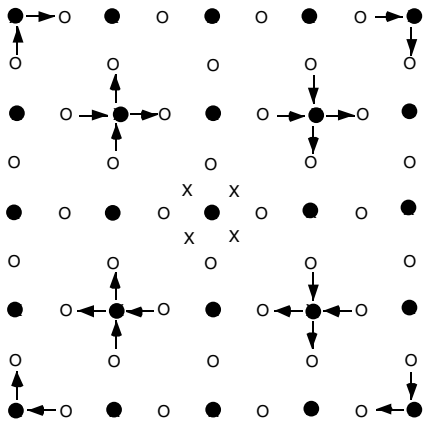

**Figure 10.** Pattern of the vector potential $A$ due to four flux tubes (crosses) carrying flux $\phi$. Black dots stand for Cu atoms and empty dots stand for O sites. The line integral of $A$ along each bond parallel to the arrow is $\frac{\phi}{2}$.

### *5.2. Triangular lattice in $W = 0$ theory*

We have also considered a symmetric triangular Hubbard lattice, which may be relevant to the newly discovered [5] $Na_xCoO_2$ superconductors which are now exciting considerable interest [69, 70]. The seven-atom centred hexagonal cluster with open boundary conditions yields no pairing for any filling. When opposite sites of this cluster are identified, one obtains a four-site cluster which is the smallest one with periodic boundary conditions. With a hopping integral $t = -1$ we find that $\tilde{\Delta}(4)$ is negative and shows a similar trend versus $U$ as in the $CuO_4$ case; the pairing energy exceeds $0.1t$ for $U \sim 4|t|$.

## 6. Superconducting flux quantization

Bulk superconductors quantize the flux through a hole in half-integer multiples of the fluxon $\phi_0$, because the quasiparticles that screen the vector potential carry charge $2e$. In finite systems the signature of superconductivity is a ground-state energy minimum at $\phi = 0$ that is separated by a barrier from a second minimum at $\phi = \phi_0/2$. With increasing size of the system, the energy (or free energy, at finite temperature) barrier separating the two minima becomes macroscopically large, and bulk superconductors can swallow up only half-integer numbers of flux quanta. As emphasized by Canright and Girvin [71], the flux dependence of the ground-state energy is definitely one of the most compelling ways of testing for superconductivity, and the existence of the two minima separated by a barrier is a strong indication of superconducting flux quantization.

### *6.1. General group theory aspects of Cu–O systems*

In the present problem, with a repulsive Hubbard model, the mechanism of attraction is driven by the $C_{4v}$ symmetry, and cannot operate in an asymmetric geometry. The flux must be inserted in such a way that the system is not distorted. In the following we consider Cu–O systems with $C_{4v}$ symmetry with respect to a central copper ion, and insert the magnetic flux in such a way that only four central triangular plaquettes feel a magnetic field (see figures 10 and 11) and the rest of the plane only experiences a vector potential.

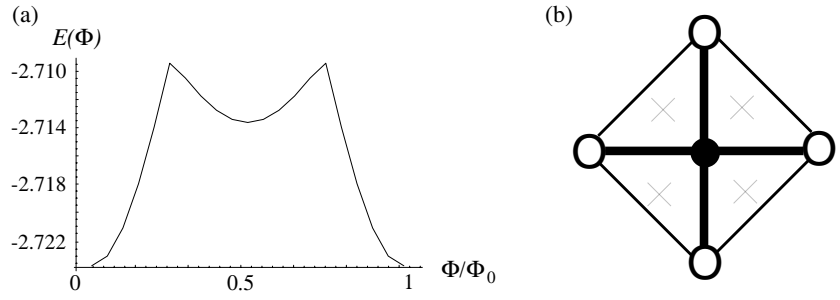


**Figure 11.** (a) Ground-state energy of the $CuO_4$ with four holes as a function of $\phi/\phi_0$. For $\phi/\phi_0$ between zero and one-quarter and between three-quarters and unity the ground state has $B_2$ symmetry; for $\phi/\phi_0$ between one-quarter and three-quarters it belongs to $A_1$. Here $t = 1$ eV, $t_{pp} = -0.01$ eV, $U = 5$ eV; $E(4, \phi)$ is in eV. (b) Topology of the $CuO_4$ cluster in the presence of $\phi$; the crosses stand for flux tubes.

Consider the pattern of figure 10. Here, the Cu sites are marked by black dots and the oxygen sites by empty dots; the X stand for tubes carrying flux $\phi$ each, symmetrically disposed around the central Cu. In accordance with the Peierls prescription we include the magnetic effects in the Hubbard model by setting

$$t_{jj'} \to t_{jj'} \exp\left(\frac{2\pi \mathrm{i}}{\phi_0} \int_j^{j'} \mathbf{A} \cdot \mathrm{d}\mathbf{r}\right),$$

where $\phi_0 = 2\pi/e$ is the flux quantum and $j$ and $j'$ are the positions of the two lattice sites connected by $t_{jj'}$. Varying $\phi$ by an integer multiple of $\phi_0$ corresponds to a gauge transformation leaving all the physical properties unchanged. The arrows help to visualize a convenient choice of the gauge at general $\phi$. Namely, running along an oriented bond in the sense of the arrow, $\int_{\to} \mathbf{A} \cdot \mathrm{d}\mathbf{r} = \frac{\phi}{2}$; along the other Cu–O bonds, not marked in the figure, $\int \mathbf{A} \cdot \mathrm{d}\mathbf{r} = 0$. One sees that in this way the flux through any closed path corresponds to the number of tubes surrounded by the path. The reflection operations of $C_{4v}$ are equivalent to $\phi \to -\phi$; reverse the directions of the arrows and for a generic $\phi$ the symmetry group reduces to $Z_4$. However, at $\phi = \frac{\phi_0}{2}$ the reversal of the magnetic field in the tubes corresponds to a jump by $\phi_0$, and this is equivalent to a gauge transformation: this implies that the symmetry group becomes larger, the new symmetry operations being reflections supplemented by a gauge transformation. Indeed, the hopping parameter $t_{jj'}$ becomes $it_{jj'}$ along the arrows, while it remains equal to $t_{jj'}$ along the unmarked bonds of figure 10(a). Any reflection operation simply changes the signs of all the hoppings along the marked bonds. Now consider the unitary transformation $S$ which changes the signs of all the Cu orbitals along both diagonals, except the central Cu. Since $S$ also has the effect of reversing all the arrows, $\sigma \times S$ is a symmetry, for all reflections $\sigma$ in $C_{4v}$. Moreover, since the product of two reflections is a rotation, the group $\tilde{C}_{4v}$ including the rotations and the reflections multiplied by $S$ is isomorphic to $C_{4v}$. The $W = 0$ pairs appropriate for half a flux quantum must involve two holes belonging to the degenerate irrep of $\tilde{C}_{4v}$. In this way, at $\phi = \frac{\phi_0}{2}$ the full symmetry is restored, allowing again for pairing and negative $\Delta$. If pairing also occurs at $\phi = \frac{\phi_0}{2}$, the superconducting flux quantization arises from a level crossing between the ground state associated with the paired state at $\phi = 0$ and the ground state associated with the paired state at $\phi = \frac{\phi_0}{2}$.

### 6.2. Application to the $CuO_4$ case and numerical results

As an illustrative application of the previous symmetry argument, let us investigate one more time the $CuO_4$ cluster. We expect that this system is a very good candidate to exhibit superconducting flux quantization, since it hosts two $W = 0$ pairs of different symmetries. As discussed above, this condition is necessary for the development of a level crossing.

In agreement with the previous prescription, we have to insert four flux tubes around the central copper (see figure 11(b)) in order to introduce a closed path around the centre, where screening currents can respond. Every O–O bond collects the Peierls phase $\frac{2\pi i}{\phi_0}\int \mathbf{A}\cdot \mathrm{d}\mathbf{r} = 2\pi i\frac{\phi}{\phi_0}$; by symmetry, $t$ is unaffected by the flux. Thus, the Hamiltonian reads as in equation (5) with

$$t_{pp} \to t_{pp}\mathrm{e}^{2\pi i\frac{\phi}{\phi_0}}.$$

We observe that a flux of the order of a fluxon in a macroscopic system would be a small perturbation; in the small cluster, however, the perturbation is small only if the hopping integral $|t_{pp}|$ is taken small compared to $t$. Numerically, the computations were performed with $t_{pp} = -0.01$ eV. By exact diagonalization, we have found that the ground-state energy $E(\phi)$ of the $CuO_4$ with four holes, as a function of $\phi$, has clearly separated minima at zero and half a flux quantum (see figure 11(a)). Furthermore, $\tilde{\Delta}(4)$ is negative both at $\phi = 0$ and $\phi_0/2$: $\tilde{\Delta}(\phi = 0) = -43$ meV and $\tilde{\Delta}(\phi = \phi_0/2) = -32$ meV.

The physical interpretation of figure 11(a) is the following. When the magnetic flux is inserted into the system, the $W = 0$ pair of $B_2$ symmetry creates a diamagnetic supercurrent that screens the external field. Such a current flows through the O–O bonds and form closed loops. As $\phi$ grows the energy of the system also increases, signalling that the $W = 0$ pair is spending its binding energy to screen the field. At a quarter fluxon a level crossing occurs, producing a second minimum at $\phi = \phi_0/2$. Here the Hamiltonian is real again and the $A_1$ pair is energetically favoured. As the flux increases further, the $A_1$ pair produces a new diamagnetic supercurrent until the initial situation is restored at $\phi = \phi_0$. The pairing states at zero flux and half a fluxon are orthogonal. There is a clear analogy with the BCS theory; in that case, the Cooper wavefunction has s symmetry and the total magnetic quantum number of the pair vanishes in the absence of flux, but not at half a flux quantum.

It is worth noting that if the Hubbard repulsion $U$ is set to zero, the second minimum at half a fluxon disappears and a trivial paramagnetic behaviour is observed. This is further evidence that the superconducting behaviour of the system is induced by repulsion.

### 6.3. Rings of symmetric clusters

We have also studied [72–74] bound pair hopping and superconducting flux quantization (SFQ) in systems with $CuO_4$ units as nodes of a graph $\Lambda$. For such systems the Hamiltonian is $H_{\mathrm{tot}} = H_0 + H_\tau$ with

$$H_0 = \sum_{\alpha\in\Lambda}\left[t\sum_{i\sigma}(d^\dagger_{\alpha\sigma}p_{\alpha,i\sigma} + p^\dagger_{\alpha,i\sigma}d_{\alpha\sigma}) + U\left(n^{(d)}_{\alpha\uparrow}n^{(d)}_{\alpha\downarrow} + \sum_i n^{(p)}_{\alpha,i\uparrow}n^{(p)}_{\alpha,i\downarrow}\right)\right],$$

while $H_\tau$ is an intercell hopping Hamiltonian. Here, $p^\dagger_{\alpha,i\sigma}$ is the creation operator for a hole on oxygen $i = 1,\ldots,4$ of the $\alpha$th cell and so on. The point symmetry group of $H_0$ includes $S_4^{|\Lambda|}$, with $|\Lambda|$ the number of nodes. We shall consider an intercell hopping which preserves the $S_4$ subgroup of $S_4^{|\Lambda|}$ in order to have $W = 0$ pair solutions.

*6.3.1. O–O hopping and SFQ.* Consider a hopping term that allows a hole in the $i$th oxygen site of the $\alpha$th unit to move towards the $i$th oxygen site of the $\beta$th unit with hopping integral $\tau_{\alpha\beta} \equiv |\tau_{\alpha\beta}|e^{i\theta_{\alpha\beta}}$:

$$H_\tau = \sum_{\alpha,\beta\in\Lambda} \sum_{i\sigma} \tau_{\alpha\beta} p^\dagger_{\alpha,i\sigma} p_{\beta,i\sigma}.$$

For $N = 2|\Lambda|$ and $\tau_{\alpha\beta} \equiv 0$, the unique ground state consists of two holes in each $CuO_4$ unit. The intercell hopping produced by small $|\tau_{\alpha\beta}| \ll |\tilde{\Delta}(4)|$ allows us to study the propagation of $p$ pairs added to a background $2|\Lambda|$ holes. When $U/t$ is such that $\tilde{\Delta}(4) < 0$, each pair prefers to lie on a single $CuO_4$ and for $N = 2|\Lambda|+2p$ the unperturbed ground state is $2^p \times \binom{|\Lambda|}{p}$ times degenerate (since each $CuO_4$ can host two degenerate $W = 0$ pairs). In the low-energy singlet sector, the problem is solved analytically to second order in $H_\tau$ and mapped into an effective Hamiltonian for $p$ hard-core bosons with a complex effective hopping integral $\mathcal{J}$ that we have calculated analytically and studied as a function of the ratio $U/t$. For ring-shaped systems, the effective model is equivalent to the Heisenberg–Ising spin chain governed by the Hamiltonian

$$H_{\rm HI} = \sum_{\alpha=1}^{|\Lambda|} \mathcal{J}\left[2\eta\sigma^z_\alpha\sigma^z_{\alpha+1} + e^{\frac{4i\pi}{|\Lambda|}\frac{\phi}{\phi_0}}\sigma^+_{\alpha+1}\sigma^-_\alpha + e^{-\frac{4i\pi}{|\Lambda|}\frac{\phi}{\phi_0}}\sigma^+_\alpha\sigma^-_{\alpha+1}\right] \tag{23}$$

where the $\sigma$ are Pauli matrices, spin up represents an empty site and spin down represents a pair. $\eta$ is the so-called anisotropy parameter and in our case $\eta = -1$. For $\eta = 1$, we have the isotropic Heisenberg interaction. By performing a Jordan–Wigner transformation, the Hamiltonian in equation (23) can also be mapped into a model of spinless fermions on the ring. In the absence of a threading magnetic field ($\phi = 0$) the problem was originally studied by Bloch [75] and then exactly solved by Hulthen [76] (in the case $\eta = -1$) and Orbach [77] (in the case $\eta \leqslant -1$) using the Bethe hypothesis [78]. A systematic analysis in the whole range of parameters was given by Yang and Yang in a self-contained series of papers [79]. Here we just recall that the model has a gapless phase if $|\eta| \leqslant 1$, corresponding to the conducting state, while an insulating phase sets in for $\eta < -1$. As in the 1D Hubbard model, the 'magnetic perturbation' ($\phi \neq 0$) does not spoil the integrability and the Heisenberg–Ising Hamiltonian remains exactly solvable by the Bethe ansatz method. Let us write an eigenfunction of $H_{\rm HI}$ as

$$a(\alpha_1, \ldots, \alpha_p) = \sum_P A_P e^{i\sum_j k_{P_j}\alpha_j}$$

where $P$ is a permutation of the integers $1, \ldots, p$ and $A_P$ are $p!$ coefficients. Shastry and Sutherland [80] have shown that the variables $k_j$ are given by

$$|\Lambda|k_j = 2\pi I_j + 4\pi\frac{\phi}{\phi_0} - \sum_{l\neq j}\theta(k_j, k_l) \tag{24}$$

with a phase shift

$$\theta(k, q) = 2\tan^{-1}\left[\frac{\eta\sin[(k-q)/2]}{\cos[(k+q)/2] - \eta\cos[(k-q)/2]}\right].$$

From equations (23) and (24) we readly see that the ground-state energy of the low-energy effective Hamiltonian $H_{\rm HI}$ is periodic with period $\phi_0/2$, independent of the number of added pairs. Thus we conclude that the purely repulsive $CuO_4$-Hubbard ring threaded by a magnetic field quantizes the flux in a superconducting fashion if the number of particles is $2|\Lambda| + 2p$ with $0 \leqslant p \leqslant |\Lambda|$.

For rings of two and three $CuO_4$ sites, we also confirmed the analytic results by exact diagonalization; for the three-$CuO_4$ ring we observed the SFQ with total number of holes

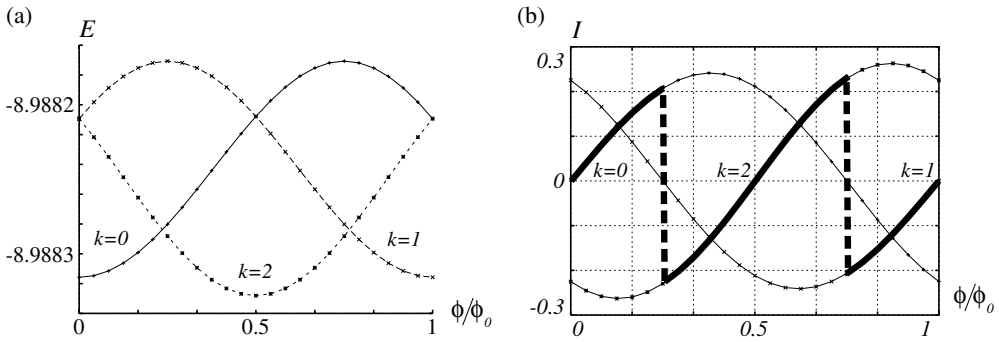


**Figure 12.** (a) Numerical results for the low-energy states of the three-$CuO_4$ ring, as a function of the concatenated magnetic flux. The energy is in units of $t$. (b) Total current for the three-$CuO_4$ ring, as a function of the magnetic flux. The current is in units of $e|\tau|/h$. In both figures, $U = 5t$, $[\tilde{\Delta}(4) \approx -0.042\,58t]$ $|\tau| = 0.001t$.

$2|\Lambda| + 2 = 8$. The switching on of the hopping $\tau$ between the oxygen sites breaks the symmetry group $C_{3v} \otimes S_4^3$ into $C_{3v} \otimes S_4$ for real $\tau$; in a magnetic field (complex $\tau$), this further breaks into $C_3 \otimes S_4$. Real $\tau$ lifts the degeneracy between the $k = 0$ subspace and the subspaces $k = 1$ and 2 of $C_3$ (as usual $k$ is related to the crystal momentum $p \equiv 2\pi\hbar k/3$ in this case), but cannot split $k = 1$ and 2 because they belong to the degenerate irrep of $C_{3v}$; complex $\tau$ resolves this degeneracy.

The three-$CuO_4$ ring is the smallest ring where we can insert a magnetic flux $\phi$ by $\tau = |\tau|e^{i\theta}$, $\theta = \frac{2\pi}{3}(\phi/\phi_0)$. The energies of the three ground-state multiplet components are reported in figure 12(a) for $|\tau| \ll |\tilde{\Delta}(4)|$ and $U = 5t$. At $\phi = 0$ the ground state belongs to the $k = 0$ subspace, while the first excited levels have $k = 1$ and 2. Their spatial degeneration is fully lifted: the $k = 1$ level increases while the $k = 2$ level decreases up to $\phi = \phi_0/2$. As $\phi$ increases, the ground-state energy grows quadratically in $\phi$ (diamagnetic behaviour). Near $\phi = \phi_0/4$ we find a level crossing between $k = 0$ and 2, while at $\phi = \phi_0/2$, $k = 0$ becomes degenerate with $k = 1$ and the ground-state energy is in a new minimum belonging to the $k = 2$ subspace: a sort of 'restoring' of the $\phi = 0$ situation is taking place as in the BCS theory [81]. Indeed, at $\phi = \phi_0/2$ the symmetry group is $\tilde{C}_{3v} \otimes S_4$ where $\tilde{C}_{3v}$ is isomorphous to $C_{3v}$ (reflections $\sigma$ are replaced by $\sigma g$, where $g$ is a suitable gauge transformation).

Fulfilling the conditions $\tilde{\Delta}(4) < 0$ and $|\tau| \ll |\tilde{\Delta}(4)|$, we have varied $U$ and $|\tau|$ and found analogous trends for the ground-state energy. Increasing $|\tau|$ with fixed $\tilde{\Delta}(4)$ lowers the central minumum and depresses the two maxima. On the other hand, if $|\tilde{\Delta}(4)|$ decreases at fixed $|\tau|$ the central minimum and the side peaks are affected in a similar way. This is reasonable since the perturbative parameter is $|\tau|/|\tilde{\Delta}(4)|$.

The current operator $\hat{I} = c\frac{\partial H_0}{\partial \phi}$ yields [82] a gauge invariant average $I$ and in figure 12(b) we display $I$ as a function of $\phi$ in the three ground-state sectors $k = 1, 2$ and 3. The current is proportional to the flux derivative of the ground-state energy (see figure 12(a)) according to the Hellmann–Feynman theorem and clearly shows a superconducting behaviour.

The ground-state energy in each $k$ sector for the non-interacting ($U = 0$) $Cu_3O_{12}$ ring shows no pairing in $CuO_4$ and indeed the ground-state energy is linear in the field at small fields (normal Zeeman effect). The lowest state is $k = 2$ throughout. The absence of SFQ is a further evidence of the repulsion-driven pairing mechanism discussed above. Thus, the dressed $W = 0$ pair screens the vector potential as a particle with an effective charge $e^* = 2e$ does. At both minima of $E(\phi)$ we have computed for the $Cu_3O_{12}$ ring $\tilde{\Delta}(8) \approx -10^{-2}t$.

*6.3.2. Cu–Cu hopping: infinite effective mass.* The three-$CuO_4$ ring with $2|\Lambda|+2=8$ holes contains a $W=0$ pair which in the case $\tilde{\Delta}(4)<0$ is bound; an intercell hopping $\tau_{\rm Cu}$ is now assumed between Cu sites only. This is perfectly able to carry a one-body current when the full system is threaded by the flux, and it does in the absence of interactions. However, the bound pairs have an interesting behaviour. $|\tau_{\rm Cu}| \ll |\tilde{\Delta}(4)|$ produces very much smaller effects on the energy than $\tau$ does, but anyhow the system behaves as a paramagnet and there is no flux-induced splitting of the three $k$ levels. This happens because the $W=0$ pair is strictly localized by the *local* symmetry. Indeed, the $S_4$ label of each $CuO_4$ unit is a good quantum number. No SFQ is observed because the screening of the magnetic field by the bound pair is forbidden. The superconducting pair behaves as if it had a very large effective mass.

## 7. $W=0$ pairing and electron–phonon interactions

The role of electron–phonon (EP) interactions in determining the superconducting correlations in the Cu–O planes of cuprates is a very controversial issue. Possibly, the pairing mechanism has a predominantly electronic origin, but many high-$T_{\rm C}$ compounds exhibit a quite noticeable doping-dependent isotope effect, suggesting that EP interactions could be important and should be included in the theory. In particular there is experimental evidence that the half breathing Cu–O bond stretching mode at $k=(\pi,0),(0,\pi)$ is significantly coupled with the doped holes in the superconducting regime and its contribution may be relevant for the $d_{x^2-y^2}$ pairing [83].

Here we further investigate this issue by addressing the question of whether the $W=0$ pairing available in the Hubbard model survives when the lattice degrees of freedom are switched on. When lattice effects are introduced in this scenario, several questions arise. In the conventional mechanism, phonons overscreen the electron repulsion; what happens if electronic screening already leads to pairing? It is not obvious that the phonons will reinforce the attraction while preserving the symmetry. More generally, some vibrations could be pairing and others pair breaking. To address these problems we use an extension of the Hubbard model in which bond stretchings dictate the couplings to the normal modes of the $C_{4v}$-symmetric configuration, generating a long-range (Fröhlich) EP interaction.

We start from the Hubbard model with on-site interaction $U$ and expand the hopping integrals $t_{i,j}(\mathbf{r}_i,\mathbf{r}_j)$ in powers of the displacements $\boldsymbol{\rho}_i$ around a $C_{4v}$-symmetric equilibrium configuration

$$t_{i,j}(\mathbf{r}_i,\mathbf{r}_j) \simeq t^0_{i,j}(\mathbf{r}_i,\mathbf{r}_j) + \sum_\alpha \left[\frac{\partial t_{ij}(\mathbf{r}_i,\mathbf{r}_j)}{\partial r_i^\alpha}\right]_0 \rho_i^\alpha + \sum_\alpha \left[\frac{\partial t_{ij}(\mathbf{r}_i,\mathbf{r}_j)}{\partial r_j^\alpha}\right]_0 \rho_j^\alpha,$$

where $\alpha = x,y$. Below, we write down the $\rho_i^\alpha$ in terms of the normal modes $q_{\eta\nu}$: $\rho_i^\alpha = \sum_{\eta\nu} S^\alpha_{\eta\nu}(i) q_{\eta\nu}$, where $\eta$ is the label of an *irrep* of the symmetry group of the undistorted system and $\nu$ is a phonon branch.

Thus, treating the Cu atoms as fixed, for simplicity, one can justify an electron–lattice Hamiltonian:

$$H_{\rm el-latt} = H_0 + V_{\rm tot}.$$

Here $H_0 = H_0^n + H_0^e$ accounts for the kinetic part of the electron–phonon system and it is given by

$$H_0 = \sum_\eta \hbar\omega_{\eta,\nu} b^\dagger_{\eta,\nu} b_{\eta,\nu} + \sum_{i,j\sigma} t^0_{i,j}(\mathbf{r}_i,\mathbf{r}_j) c^\dagger_{i\sigma} c_{j\sigma};$$

the $\omega$ are normal mode frequencies. The interacting part $V_{\rm tot} = V + W$ contains the Hubbard repulsion $W$ and the electron–phonon interaction $V$. The latter can be written in terms of the

parameters $\xi_{\eta,\nu} = \lambda_{\eta\nu}\sqrt{\frac{\hbar}{2M\omega_{\eta,\nu}}}$, where the $\lambda$ are numbers of order unity that modulate the EP coupling strength, while $M$ is the oxygen mass. Then,

$$V = \sum_{\eta,\nu} \xi_{\eta,\nu}(b^{\dagger}_{\eta,\nu} + b_{\eta,\nu})H_{\eta,\nu},$$

and the $H_{\eta,\nu}$ operators are given by

$$H_{\eta,\nu} = \sum_{i,j}\sum_{\alpha,\sigma}\left\{S^{\alpha}_{\eta\nu}(i)\left[\frac{\partial t_{ij}(\mathbf{r}_i,\mathbf{r}_j)}{\partial r^{\alpha}_i}\right]_0 + S^{\alpha}_{\eta\nu}(j)\left[\frac{\partial t_{ij}(\mathbf{r}_i,\mathbf{r}_j)}{\partial r^{\alpha}_j}\right]_0\right\}(c^{\dagger}_{i,\sigma}c_{j,\sigma} + \text{h.c.}).$$

This is physically more detailed than the Hubbard–Holstein model, where electrons are coupled to a local Einstein phonon and the superconducting phase has been investigated in detail [84, 85]. Indeed, in the present context the Hubbard–Holstein model is not fully satisfactory because it is restricted to on-site EP couplings, which would be impaired by a strong Hubbard repulsion. On the other hand, the use of Fröhlich-like phonons was suggested [86–88] for modelling the Cu–O planes in the strong-EP-coupling regime: a long-range EP coupling removes the problem of polaron self-trapping, otherwise present in the case of the Holstein interaction, where an unphysically large polaron (and bipolaron) mass occurs.

By generalizing to $H_{\text{el}-\text{latt}}$ the canonical transformation proposed for the electronic part $H = H^{e}_{0} + W$, one can derive [89, 90] an effective interaction between the particles in the pair. We obtained a new Cooper-like equation $H_{\text{pair}}|\varphi\rangle = E|\varphi\rangle$ with an effective two-body Hamiltonian, acting upon the dressed $W = 0$ pair $|\varphi\rangle$. As in section 3 the pairing criterion involves the properly renormalized Fermi energy $E^{(\text{R})}_{\text{F}}$: if the lowest-energy eigenvalue $E$ is such that $E = E^{(\text{R})}_{\text{F}} + \Delta$ with negative $\Delta$, the dressed $W = 0$ pair is bound in the many-body interacting problem and the system undergoes a Cooper instability. We observed that this extended approach is very accurate at weak coupling and is also qualitatively predictive in the intermediate-coupling regime.

As an illustrative application we focused again on $CuO_4$. This cluster represents a good test of the interplay between electronic and phononic pairing mechanisms since we can compare exact diagonalization results with the analytic approximations of the canonical transformation. $CuO_4$ allows only the coupling to phonons at the centre or at the edge of the Brillouin zone; however, phonons near the edge are precisely the most relevant ones [83]. We recall (see section 2.2) that the pure Hubbard $CuO_4$ cluster with O–O hopping $t_{pp} = 0$ yields $\tilde{\Delta}(4) < 0$, and a degenerate $W = 0$ bound pair with $A_1$ and $B_2$ components. A standard Jahn–Teller calculation in which the degenerate ground-state wavefunctions interact with the vibrations predicts distortions that already at moderate EP coupling destroy the pairing [90]. We also explored the scenario beyond this approximation. The analytical solution of the Cooper-like equation shows that the electronic pairing is enhanced by the phonon contribution. In particular the binding energy of the pair in the $B_2$ symmetry channel increases more rapidly than in the $A_1$ channel.

In order to go beyond the weak-coupling regime we have exactly diagonalized the Hamiltonian in a truncated Hilbert space. We obtained several indications. First, the catastrophic distortions predicted by the Jahn–Teller approximation are not borne out by more complete approaches involving a broader spectrum of electronic states. Pairing also prevails at strong coupling in part of the parameter space, in the symmetry channels where $W = 0$ pairs occur. The correct trend is predicted by the canonical transformation approach, which also explains the pairing or pair-breaking character of the individual normal modes. In particular it is found that the half-breathing modes give a synergic contribution to the purely electronic pairing; since they are believed to be mainly involved in optimally doped cuprates, our findings suggest a joint mechanism, with the Hubbard model that captures a crucial part of the physics.

## 8. Conclusions and outlook

We have presented the following evidence that the $W = 0$ pairs are the quasi-particles that, once dressed, play the role of Cooper pairs.

(1) As two-body states they do not feel the large on-site repulsion, that would come in first-order perturbation in any theory of pairing with any other kind of pairs.
(2) The indirect interaction with the background particles gives attraction, and bound states with physically appealing binding energies.
(3) The same results are also borne out by exact diagonalization in finite clusters, if and only if they have the correct symmetry and filling to give rise to $W = 0$ pairs in partially filled shells.
(4) Both in clusters and in the plane, the superconducting flux quantization results from the symmetry properties of $W = 0$ pairs.

The set-up of our theory of the effective interaction $W_{\rm eff}$ between two holes (or electrons) is quite general; although we developed it in detail for Hubbard models, it is well suited to be extended in order to include other ingredients, like phonons. In principle we can obtain $W_{\rm eff}$ by our canonical transformation, including systematically any kind of virtual intermediate states. The closed-form analytic expression of $W_{\rm eff}$ we obtained includes four-body virtual states. This describes repeated exchange of an electron–hole pair to all orders. One can envisage the pairing mechanism by spin-flip exchange diagrams that are enhanced by the $C_{4v}$ symmetry. The argument does not depend in any way on perturbation theory, and the equations retain their form, with renormalized parameters, at all orders. We find that in the three-band Hubbard model ${}^1A_2$ pairs are more tightly bound close to half filling, but ${}^1B_2$ pairs are favoured when the filling increases. Here, as in the BCS theory, the superconducting flux quantization relies on the existence of bound pairs of different symmetries. We recall, however, that these symmetry labels are not absolute, but depend on the choice of a gauge convention. We get attraction and pairing at all fillings we have considered (above half filling), but the binding energy of the ${}^1A_2$ pairs drops by orders of magnitude as the filling increases. The three-band Hubbard model might be too idealized to allow a detailed quantitative comparison with experiments; however, some qualitative answers are very clear.

Using the Lieb theorem [23] and a symmetry analysis based on the $W = 0$ theorem, one can fix the way the interactions remove the high degeneracy of the Hubbard model at half filling. This can be used to study pairing in the doped system by the above canonical transformation. Exact numerical data on the $4 \times 4$ square lattice are available [30], and this allows us to test the $W = 0$ pairing mechanism within the one-band Hubbard model, improving over previous weak-coupling analyses [45, 46]. For a full application of the $W = 0$ theorem, we had to include non-trivial symmetries which are not isometries; this enabled us to classify the $W = 0$ channels and calculate the binding energies analytically. Once the analysis is so complete, the criteria for pairing are unambiguous. Moreover, the success of the weak-coupling approach has been noted by other authors [91], and the reason is fully clarified by the $W = 0$ theory.

Despite some evident and important differences that we have pointed out above, our mechanism can broadly speaking be thought of as a lattice realization of the pioneering one proposed long ago [12] by Kohn and Luttinger. The repulsion is avoided by the $W = 0$ configuration mixing without using parallel spins and high angular momenta. The basic source of attraction, however, is essentially the same, since in second order, in the singlet channel, the spin-flip diagram is the only one that survives. We found pairing in the singlet channel in a variety of models including carbon nanotubes [66]. This real-space approach is suitable for realizing thought experiments, like those involving the SFQ (section 6).

On the other hand, the above results also prove that important ingredients are still missing and must be included. The $4 \times 4$ model shows evidence of bound pairs of non-vanishing momentum, in degenerate representations. This opens up the possibility of charge inhomogeneities and Jahn–Teller distortions. However, modelling vibration effects in a $CuO_4$ cluster we find that the outcome depends on which phonon mode is most strongly coupled. The bound pairs can be flexible enough to prevent distortions and actually gain binding energy in the presence of $A$ and $B$ phonons, whilst $E$ vibrations are definitely pair breaking.

## References


[1] Bednorz J G and Müller K A 1986 *Z. Phys.* B **64** 189
[2] Schn J H, Kloc Ch, Haddon R C and Batlogg B 2000 *Science* **288** 656
[3] Tang Z K, Zhang L, Wang N, Zhang X X, Wen G H, Lee G D, Wang J N, Chan C T and Sheng P 2001 *Science* **292** 2462
[4] Maeno Y *et al* 1994 *Nature* **372** 532
[5] Takada K, Sakurai H, Takayama-Muromachi E, Izumi F, Dilanian R A and Sasaki T 2003 *Nature* **422** 53
[6] Hubbard J 1963 *Proc. R. Soc.* A **276** 238
Hubbard J 1964 *Proc. R. Soc.* A **277** 237
Hubbard J 1964 *Proc. R. Soc.* A **281** 401
[7] Bickers N E, Scalapino D J and White S R 1987 *Int. J. Mod. Phys.* **1** 687
[8] Yanase Y, Jujo T, Nomura T, Ikeda H, Hotta T and Yamada K 2003 *Phys. Rep.* **387** 1–149
[9] For a review on the $t$–$J$ Model see, e.g. Dagotto E 1994 *Rev. Mod. Phys.* **66** 763
[10] Sushkov O P 1996 *Phys. Rev.* B **54** 9988 and reference therein
Flambaum V V, Kuchiev M Y and Sushkov O P 1994 *Physica* C **235–240** 2218
[11] Gutzwiller M C 1963 *Phys. Rev. Lett.* **10** 159
[12] Kohn W and Luttinger J M 1965 *Phys. Rev. Lett.* **15** 524
[13] Shankar R 1994 *Rev. Mod. Phys.* **66** 129
[14] Chubukov A V 1993 *Phys. Rev.* B **48** 1097
[15] Bickers N E, Scalapino D J and White S R 1989 *Phys. Rev. Lett.* **62** 961
Monthoux P, Balatsky A and Pines D 1991 *Phys. Rev. Lett.* **67** 3448
Bickers N E and White S R 1991 *Phys. Rev.* B **43** 8044
[16] Zanchi D and Schulz H J 1996 *Phys. Rev.* B **54** 9509
Zanchi D and Schulz H J 2000 *Phys. Rev.* B **63** 13609
[17] Halboth C J and Metzner W 2000 *Phys. Rev. Lett.* **61** 7364
[18] Honerkamp C and Salmhofer M 2001 *Phys. Rev. Lett.* **64** 184516
[19] Anderson P W, Baskaran G, Zou Z and Hsu T 1987 *Phys. Rev. Lett.* **58** 2790
[20] Anderson P W and Zou Z 1988 *Phys. Rev.* **60** 132
[21] Su G and Suzuki M 1998 *Phys. Rev.* B **58** 117
[22] Lieb E H and Wu F Y 1968 *Phys. Rev. Lett.* **20** 1445
[23] Lieb E H 1989 *Phys. Rev. Lett.* **62** 1201
[24] Nagaoka Y 1966 *Phys. Rev.* **147** 392
[25] Mielke A 1991 *J. Phys. A: Math. Gen.* **24** L73
Mielke A 1992 *J. Phys. A: Math. Gen.* **25** 4335
Mielke A 1992 *Phys. Lett.* A **174** 443
[26] Tasaki H 1992 *Phys. Rev. Lett.* **69** 1608
Tasaki H 1989 *Phys. Rev.* B **40** 9192
[27] Richardson R W 1966 *Phys. Rev.* **141** 949
[28] Balseiro C A, Rojo A G, Gagliano E R and Alascio B 1988 *Phys. Rev.* B **38** 9315
[29] Zhang S, Carlson J and Gubernatis J E 2000 *Phys. Rev. Lett.* **84** 2550
[30] Fano G, Ortolani F and Parola A 1990 *Phys. Rev.* B **42** 6877
Parola A, Sorella S, Parrinello M and Tosatti E 1991 *Phys. Rev.* B **43** 6190
Fano G, Ortolani F and Parola A 1992 *Phys. Rev.* B **46** 1048
Fano G, Ortolani F and Semmeria F 1990 *Int. J. Mod. Phys.* B **3** 1845
[31] Cini M and Balzarotti A 1996 *Nuovo Cimento* D **18** 89
[32] Hirsch J E, Tang S, Loh E and Scalapino D J 1988 *Phys. Rev. Lett.* **60** 1668
[33] Hirsch J E, Tang S, Loh E and Scalapino D J 1989 *Phys. Rev.* B **39** 243
[34] Ogata M and Shiba H 1988 *J. Phys. Soc. Japan* **57** 3074

[35] Martin R L 1996 *Phys. Rev.* B **14** R9647
[36] Emery V J and Reiter G 1988 *Phys. Rev.* B **38** 4547
[37] Fulde P 1991 *Electron Correlation in Molecules and Solids* (*Springer Series in Solid State Sciences* vol 100) (Berlin: Springer)
[38] Hybertsen M S, Schlüter M and Christensen N 1988 *Phys. Rev.* B **39** 9028
Schlüter M 1990 *Superconductivity and Applications* ed H S Kwok *et al* (New York: Plenum) p 1
[39] Zhang F C and Rice T M 1988 *Phys. Rev.* B **37** 3759
[40] Cini M and Balzarotti A 1997 *Solid State Commun.* **101** 671
Cini M, Balzarotti A, Tinka Gammel J and Bishop A R 1997 *Nuovo Cimento* D **19** 1329
[41] Cini M, Balzarotti A and Stefanucci G 2000 *Eur. Phys. J.* B **14** 269
[42] Cini M and Balzarotti A 1997 *Phys. Rev.* B **56** 14711
[43] Cini M, Balzarotti A, Brunetti R, Gimelli M and Stefanucci G 2000 *Int. J. Mod. Phys.* B **14** 2994
[44] Metzner W and Vollhardt D 1989 *Phys. Rev.* B **39** 4462
[45] Friedman B 1991 *Europhys. Lett.* **14** 495
[46] Galan J and Verges J A 1991 *Phys. Rev.* B **44** 10093
[47] Cini M, Stefanucci G and Balzarotti A 1999 *Eur. Phys. J.* B **10** 293
[48] Cini M, Stefanucci G and Balzarotti A 1999 *Solid State Commun.* **109** 229
[49] Cini M, Balzarotti A and Stefanucci G 1998 *Preprint* cond-mat/9811116
[50] Shen Z X, Spicer W E, King D M, Dessau D S and Wells B O 1995 *Science* **267** 343 and references therein
[51] Lynch D W and Olson C G 1999 *Photoemission Studies of High-Temperature Superconductors* (Cambridge: Cambridge University Press)
[52] Stefanucci G and Cini M 2002 *Phys. Rev.* B **66** 115108
[53] Shen S Q, Qiu Z M and Tian G S 1994 *Phys. Rev. Lett.* **72** 1280
[54] Cini M and Stefanucci G 2001 *Solid State Commun.* **117** 451
[55] Cini M and Stefanucci G 2001 *J. Phys.: Condens. Matter* **13** 1279
[56] Moreo A and Dagotto E 1990 *Phys. Rev.* B **41** 9488
[57] Bonca J, Prelovsek P and Sega I 1989 *Phys. Rev.* B **39** 7074
[58] Hasegawa Y and Poilblanc D 1989 *Phys. Rev.* B **40** 9035
[59] Cini M, Perfetto E and Stefanucci G 2001 *Eur. Phys. J.* B **20** 91
[60] Belash J T, Zharikov O V and Pal'nichenko A V 1987 *Solid State Commun.* **63** 153
Belash J T, Bronnikov A D, Zharikov O V and Pal'nichenko A V 1987 *Solid State Commun.* **64** 1445
Belash J T, Bronnikov A D, Zharikov O V and Pal'nichenko A V 1989 *Solid State Commun.* **69** 921
[61] Bockrath M, Hone J, Zettl H, McEuen P L, Rinzler A G and Smalley R E 2000 *Phys. Rev.* B **61** R10606
[62] Gao B, Kleinhammes A, Tang X P, Bower C, Fleming L, Wu Y and Zhou O 1999 *Chem. Phys. Lett.* **307** 153
Zhao J, Buldum A, Han J and Ping Lu J 2000 *Phys. Rev. Lett.* **85** 1706
[63] Zhao J *et al* 2000 *Phys. Rev. Lett.* **85** 1706
[64] Balents L and Fisher M P A 1997 *Phys. Rev.* B **55** R11973
[65] Sólyom J 2000 *Proc. School and Workshop on Nanotubes and Nanostructures (Santa Margherita di Pula (Ca), Italy)*
[66] Perfetto E, Stefanucci G and Cini M 2002 *Phys. Rev.* B **66** 165434
Perfetto E, Stefanucci G and Cini M 2001 *Eur. Phys. J.* B **30** 139
[67] Lopez Sancho M P, Munoz M C and Chico L 2001 *Phys. Rev.* B **63** 165419
[68] Tchougreef A L and Hoffman R 1992 *J. Phys. Chem.* **96** 8993
[69] Lorenz B, Cmaidalka J, Meng R L and Chu C W 2003 *Phys. Rev.* B **68** 132504
[70] Chou F C, Cho J H, Lee P A, Abel E T, Matan K and Lee Y S 2004 *Phys. Rev. Lett.* **92** 157004
[71] Canright G S and Girvin S M 1989 *Int. J. Mod. Phys.* B **3** 1943
[72] Cini M, Stefanucci G, Perfetto E and Callegari A 2002 *J. Phys.: Condens. Matter* **14** L709
[73] Callegari A, Cini M, Perfetto E and Stefanucci G 2003 *Eur. Phys. J.* B **34** 455
[74] Callegari A, Cini M, Perfetto E and Stefanucci G 2003 *Phys. Rev.* B **68** 153103
[75] Bloch F 1930 *Z. Phys.* **61** 206
Bloch F 1932 *Z. Phys.* **74** 295
[76] Hulthen L 1938 *Ark. Mat. Astron. Fysik* **26A** (1)
[77] Orbach R 1958 *Phys. Rev.* **112** 309
[78] Bethe H A 1931 *Z. Phys.* **71** 205
[79] Yang C N and Yang C P 1966 *Phys. Rev.* **147** 303
Yang C N and Yang C P 1966 *Phys. Rev.* **150** 321
Yang C N and Yang C P 1966 *Phys. Rev.* **150** 327
Yang C N and Yang C P 1966 *Phys. Rev.* **151** 258

[80] Shastry B S and Sutherland B 1990 *Phys. Rev. Lett.* **65** 243
Sutherland B and Shastry B S 1990 *Phys. Rev. Lett.* **65** 1833
[81] Little W A and Parks R D 1962 *Phys. Rev. Lett.* **9** 9
[82] Kohn W 1964 *Phys. Rev.* **133** A171
[83] Shen Z X, Lanzara A, Ishihara S and Nagaosa N 2002 *Phil. Mag.* B **82** 1349–68
[84] Pao C H and Schuttler H B 1998 *Phys. Rev.* B **57** 5051
Pao C H and Schuttler H B 1999 *Phys. Rev.* B **60** 1283
[85] Alexandrov A S 1992 *Phys. Rev.* B **46** 2838
Wellein G, Roder H and Fehske H 1996 *Phys. Rev.* B **53** 9666
Bonca J, Katrasnik T and Trugman S A 2000 *Phys. Rev. Lett.* **84** 3153
[86] Alexandrov A S and Kornilovitch P E 2002 *J. Phys.: Condens. Matter* **14** 5337
[87] Alexandrov A S 2003 *Int. J. Mod. Phys.* B **17** 3315
[88] Bonca J and Trugman S A 2001 *Phys. Rev.* B **64** 094507
[89] Perfetto E and Cini M 2004 *Phys. Rev.* B **69** 92508
[90] Perfetto E and Cini M 2004 *J. Phys.: Condens. Matter* **16** 4845
[91] Kondo J 2001 *J. Phys. Soc. Japan* **70** 808